



**NIST Internal Report
NIST IR 8533**

Traceable Comparisons of Water-Triple-Point Cells

*Traceability of NIST Water-Triple-Point Cells to the CCT-K7.2021
CIPM Key Comparison*

Weston L. Tew

This publication is available free of charge from:
<https://doi.org/10.6028/NIST.IR.8533>

NIST Internal Report
NIST IR 8533

Traceable Comparisons of Water-Triple-Point Cells

*Traceability of NIST Water-Triple-Point Cells to the CCT-K7.2021
CIPM Key Comparison*

Weston L. Tew
Sensor Science Division
Physical Measurement Laboratory

This publication is available free of charge from:
<https://doi.org/10.6028/NIST.IR.8533>

November 2024



U.S. Department of Commerce
Gina M. Raimondo, Secretary

National Institute of Standards and Technology
Laurie E. Locascio, NIST Director and Under Secretary of Commerce for Standards and Technology

NIST IR 8533
November 2024

Certain commercial equipment, instruments, software, or materials, commercial or non-commercial, are identified in this paper in order to specify the experimental procedure adequately. Such identification does not imply recommendation or endorsement of any product or service by NIST, nor does it imply that the materials or equipment identified are necessarily the best available for the purpose.

NIST Technical Series Policies

[Copyright, Use, and Licensing Statements](#)

[NIST Technical Series Publication Identifier Syntax](#)

Publication History

Approved by the NIST Editorial Review Board on 2024-07-31

How to Cite this NIST Technical Series Publication

Weston L. Tew (2024) Traceable Comparisons of Water-Triple-Point Cells. (National Institute of Standards and Technology, Gaithersburg, MD), NIST Internal Report (IR) NIST IR 8533. <https://doi.org/10.6028/NIST.IR.8533>

Author ORCID iDs

Weston Tew: 0000-0002-9979-9136

Contact Information

weston.tew@nist.gov

Abstract

A specific sub-set of comparison data are presented for two NIST water-triple-point cells that provide traceability to the results of the recent Consultative Committee for Thermometry CCT-K7.2021 CIPM Key Comparison of Water-Triple-Point Cells. NIST had initially been an official participant in the CCT-K7.2021 but later withdrew from the comparison after the breakage of two NIST transfer cells. Despite this status as a withdrawn former participant, enough NIST data were taken prior to and during the comparison to provide a direct link to the results of the K7.2021 using the measurements on a NIST transfer cell performed by the Pilot Laboratory, the National Research Council of Canada (NRC). The NIST data were obtained from routine scale maintenance and research activities, and hence did not conform to the official protocol of the CCT-K7.2021. Nonetheless, these data are of good quality and sufficient to establish an overall uncertainty of less than 0.1 mK in the temperature difference of a NIST reference WTP cell relative to the CCT-K7.2021 Key Comparison Reference Value (KCRV). This linkage is sufficient to provide evidence of traceability to the CCT-K7.2021 and supports NIST Quality System requirements for thermometric standards under the ISO 17025(2017).

Keywords

Consultative Committee on Thermometry; Fixed Point Cells; International Comparisons; International Temperature Scale; kelvin; Temperature Standards; Water Triple Point.

Table of Contents

1. Introduction	1
2. The water triple point	2
2.1. Water triple point cells metrology and commercial development.....	2
2.2. The water isotopic composition and revised definitions.....	6
2.3. The use of water triple point cells at NBS/NIST	7
3. The CCT international comparisons for the water triple point	9
3.1. BIPM international comparison of triple point of water cells (1994-1995).....	9
3.2. CCT-K7 (2002-2004)	9
3.3. CCT-K7.2021 (2021-2022)	11
4. Experimental systems and results at NIST	16
4.1. Comparison of water triple point cells in the NIST LTCF.....	16
4.2. WTP cell Comparisons for the Boltzmann constant determination	18
4.3. Experimental procedures.....	18
4.4. NIST WTP Data	20
4.5. Data Summaries and Analysis.....	23
5. Linking the NIST comparison data to the CCT-K7.2021 results	28
5.1. Corrections.....	28
5.2. Uncertainties.....	30
5.3. Final Results and Discussion.....	37
6. Conclusions	39
References	40
Appendix A. NIST Certificate of Analysis for the NIST transfer cell s/n 1454Q	1
A.1. Uncertainty budget for direct comparison of the NIST Thermodynamic Metrology Group water triple point cell (Isotech Model B13-65-270Q, s/n 1454) with one of the NIST reference water triple point cells (s/n A-Q5009)	5
A.2. Uncertainty budget for the realization of a NIST reference water triple point cell (s/n A-Q5009)...	6
Appendix B. Report of Isotopic Analysis for NIST transfer cell s/n 1454Q	1
Appendix C. Report of Isotopic Analysis for NIST reference cell s/n Q1034	1

List of Tables

Table 1 A partial reproduction of Table 4.6 ‘Results of Batch IV’ from the K7.2021 Report including resistance data for the NIST1454Q.[2]	14
Table 2 A partial reproduction of Table 4.6 ‘Results of Batch IV’ in the K7.2021 Report including temperature difference data for the NIST1454Q.[2]	15
Table 3 Summary information for the WTP cells used by NIST for this study.	16

Table 4 The usage history of the WTP cells Q1034 and 1454Q in the NIST LTCF from 2017 through 2022. The dates shown are those associated with the initiation of various ice mantles which are given labels as shown in the two cells' columns. Also shown are other dates associated with each cell's history (see text).	17
Table 5 Information mapping the SPRTs and cell mantles used as the basis for the comparison results.	17
Table 6 The measurement distribution for the SPRTs and Ice Mantles reported here.	19
Table 7. Procedures and data specified in the K7.2021 protocol and as provided in this work.....	19
Table 8 A summary of the NIST LTCF data for the differences between the transfer and reference cells.	24
Table 9 The GMMN-weighted mean parameters for averaging the SPRT data.	25
Table 10 A parsing of the data into two halves before and after the 2020 data lapse.	26
Table 11. The GMMN-weighting parameters for averaging the time-segmented SPRT data.....	27
Table 12 Isotopic information for the NIST transfer and reference WTP cells.	29
Table 13 Uncertainty budget for this study in the K7.2021 format of standard uncertainties.	36
Table 14 A summary of the temperature difference results obtained for this study.....	37

List of Figures

Figure 1 Water triple point cells showing the two most common design types with regions of solid, liquid and vapor phase water contained in sealed glass envelopes. (Credit: ASTM international)	4
Figure 2. A reproduction of data from the CCT-K7.2021 comparison batch IV during February and March of 2022, including data from the NIST replacement transfer cell 1454Q. Data are expressed in terms of temperature differences with respect to the NRC reference cells. Data from two separate ice mantles are shown, with the second mantle series starting on Feb 21.	12
Figure 3. Examples of capsule-type SPRTs as adapted into glass tubing for immersion use in WTP cells. A.) 9.0 mm ID / 11.0 mm OD probe for accommodating traditional capsule-type models. B.) 5.8 mm ID /7.6 mm OD probe for accommodating low-profile capsule models. C.) traditional-style capsule SPRT with Pt sheath intact. D.) traditional-style capsule SPRT with Pt sheath removed.	20
Figure 4 WTP zero-power resistance data from capsule SPRT 1774092	21
Figure 5 Time series data for Series D2 , mantles 21A-1 and 21A-2, April 9, 2021. a). SPRT 56860103 in Q1034 and later moved to 1454Q. b). SPRT 162D3363 in cell 1454Q and then moved into cell Q1034.	23

Preface

The purpose of this report is to provide documentation to support traceability at NIST to the results of the Consultative Committee on Thermometry K7.2021 comparison of water triple point cells. These results are in lieu of official participation in the K7.2021 and serve to support quality system requirements at NIST under the requirements of the ISO 17025 laboratory calibration competence standard. The report provides background and context on the K7.2021 specific to NIST, including a partial history of NIST/NBS usage of water triple point cells and NIST participation in past international comparisons over the last several decades. The report can serve as an interim document demonstrating a level of traceability to the K7.2021 until such time that NIST is able to participate in other bilateral comparisons that may supersede these results.

Acknowledgments

The author wishes to thank Dr Andrea Peruzzi of the National Research Council of Canada for assistance in understanding certain aspects of the CCT-K7.2021 comparison and reviewing the manuscript. The author thanks Klaus Quelhas of Theiss Research and Antonio Possolo, NIST Fellow, for their reviews of the manuscript.

1. Introduction

The water triple point (WTP) is a thermometric fixed point central to the definitions used in the International Temperature Scale of 1990 (ITS-90) [1] and served as the definition of the SI unit of temperature, the kelvin, from 1954 to 2019. The Consultative Committee for Thermometry (CCT) of the International Committee for Weights and Measures (CIPM) approved a key comparison study for water triple point cells beginning in 2021 designated as the CCT-K7.2021[2]. This comparison was piloted by the National Research Council of Canada (NRC) and was essentially an extension of an earlier CCT key comparison then designated as CCT-K7 [3]. The original CCT-K7 had been conducted by the Bureau International de Poids et Mesures (BIPM) between 2004 and 2006 with 20 national metrology institute (NMI) participants. Both studies had similar objectives: to perform a series of comparisons of high-quality WTP ‘transfer’ cells ; and to thereby enable an indirect comparison of the various ‘national standard’ WTP cells as maintained at each of the participants’ institutes. The results were tabulated in the form of temperature differences between pairs of cells as determined by standard platinum resistance thermometers (SPRTs). Temperature differences were then calculated between each of the participants’ transfer cells and between the participants’ national WTP cell references versus a single key comparison reference value (KCRV).

The CCT-K7.2021 recently concluded and the final report has been published [2]. Each of the original 19 participating NMIs submitted a transfer WTP cell to be compared at the NRC. NIST was among the original 20 participants and submitted a transfer WTP cell to the NRC for the purposes of the comparison. That cell was lost due to an accidental breakage at the NRC in November of 2021. This breakage occurred before any pilot comparison data could be obtained using that cell. NIST then sent a replacement transfer cell in December of 2021 which was received at the NRC and a full set of comparison data was obtained using this replacement cell. Once returned to NIST, this cell then suffered an unrecoverable breakage in June of 2022, precluding any further use of the cell for the CCT-K7.2021. NIST then asked to withdraw from the comparison and the participants agreed with the request. Nonetheless, the comparison data that was obtained at the NRC using the NIST replacement cell was still published in the final report [2]. The use of that NRC comparison data combined with other NIST data obtained using the replacement cell prior to the CCT-K7.2021 allows a traceable link to the K7.2021 results and is the subject of this report.

2. The water triple point

The water triple point is defined as the value of temperature and pressure for which a thermal and phase equilibrium exists for vapor, liquid and solid forms of chemically pure water. The three-phase equilibrium conveys a thermodynamic state of the highest stability as predicted by the Gibbs phase rule, for which the degrees of freedom $f=c-p+2=0$ for phases $p=3$, and chemical components $c=1$. The phase rule predicts stability in the sense that $f=0$ means that no intensive variables are needed to describe the thermodynamic state of the water. In other words, the pressure and temperature are intrinsic properties of the system and do not need to be measured or specified to uniquely determine the thermodynamic state. The triple point pressure p_{wtp} can be measured and is known via the IAPWS-95 formulation [4], $p_{\text{wtp}} = 611.657$ (0.010) Pa. The triple point temperature was first measured by Stimson [5] to be 0.010 °C above the normal melting point temperature (melting point of pure ice water under 101.325 kPa of pressure). From 1954 to 2019 the WTP temperature served to define the unit kelvin under the International System (SI) of units for which $T_{\text{wtp}} \equiv 273.16$ K. Moreover, the WTP has served as an indispensable fixed point reference temperature for the purposes of defined interpolation in various international temperature scales since the IPTS-48 and continues to serve that role today in the ITS-90.

2.1. Water triple point cells metrology and commercial development

The early development of WTP cells at the National Bureau of Standards (NBS) occurred during the 1930s as led by [Harold Stimson](#). Stimson's work on the thermodynamic properties of water and steam remained unpublished until 1945 [5]. The WTP temperature and cells for its realization came into wider use with the advent of the International Practical Temperature Scale (IPTS) of 1948. Later, (the late 1950s) a commercial laboratory was established in Wheaton Maryland (MD) by a former NBS technician, James L. Cross [6], for the production of cells with two standardized designs, the so-called 'Type A' and 'Type B' WTP cells (see Figure 1). These cells were known under the 'Jarrett' brand¹, made from borosilicate glass and filled with purified water undergoing multiple stages of distillation. At the time, the primary challenges were removing soluble impurities from interior glass surfaces and removing all air from the water prior to sealing the glass.

A study was published by the NBS in 1982 [7] which examined the reproducibility of a sampling of 21 type A and B Jarrett WTP cells made between 1958 and 1981. All but one of these cells yielded realization temperatures between +0.013 mK and -0.094 mK with respect to the

¹ Disclaimer: Certain equipment, instruments, software, or materials are identified in this paper in order to specify the experimental procedure adequately. Such identification is not intended to imply recommendation or endorsement of any product or service by NIST, nor is it intended to imply that the materials or equipment identified are necessarily the best available for the purpose.

average temperature from a collection of four relatively new reference cells. This study established a nominal uncertainty of ~ 0.05 mK for the use of these cells.

The Wheaton MD facility served as the near-exclusive source for WTP cells used at NBS and later at NIST from the late 1950s through 1996 when the facility closed and the remaining stock and equipment were sold off. Isothermal Technologies Ltd assumed the remaining inventory, Intellectual Property and rights to the trade name 'Jarrett' at that time. Meanwhile, other commercial sources for high-quality WTP cells were emerging and the ASTM published a consensus standard guide for the use of WTP cells in 1995 where the standardized designs for the Type A and Type B cells were adopted [8]. More recent design variations have also emerged, including a modified version of the Type B with an additional bottom-center seal-off port (e.g. sometimes referred to as 'Type C').

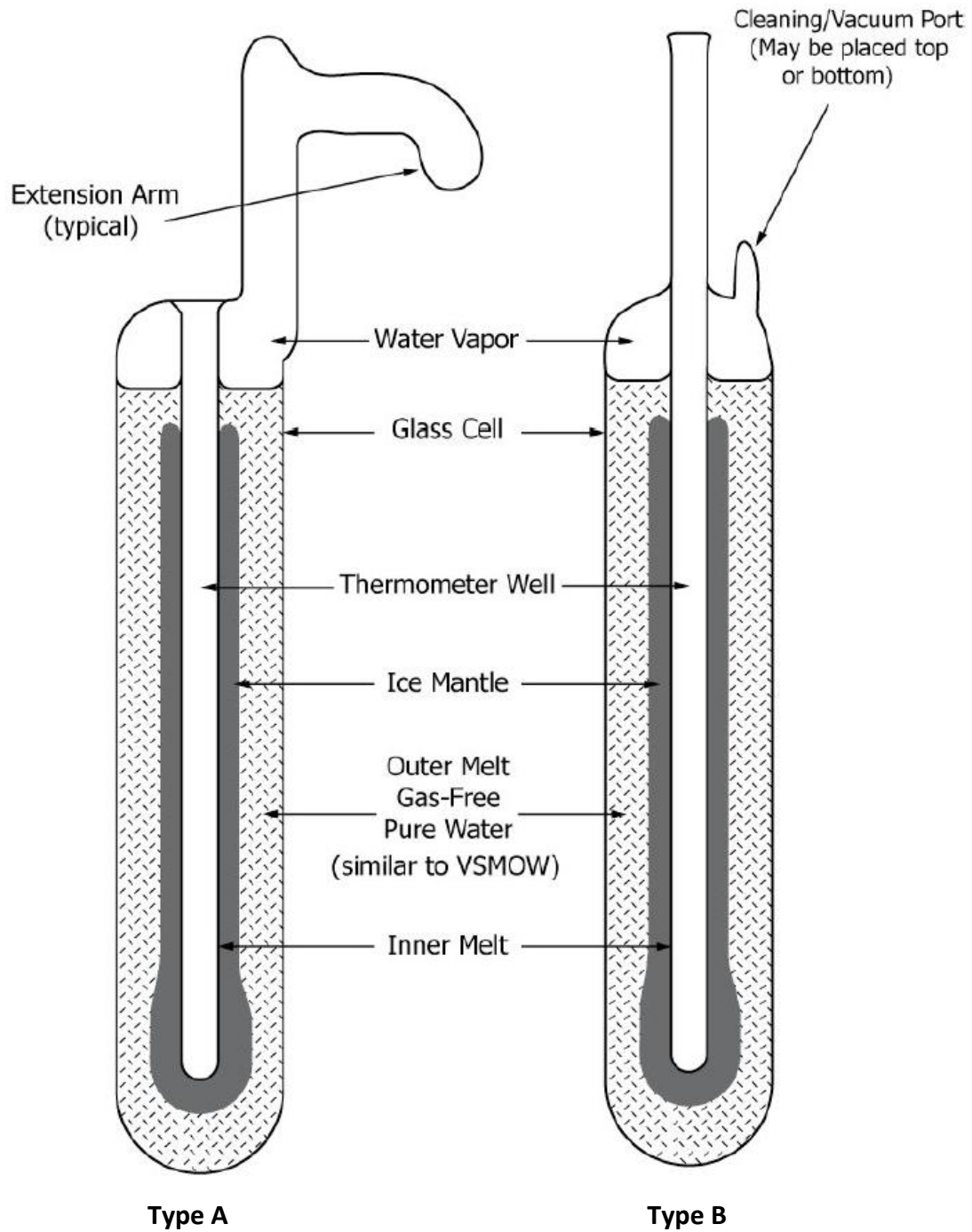


Figure 1 Water triple point cells showing the two most common design types with regions of solid, liquid and vapor phase water contained in sealed glass envelopes. (Credit: ASTM international)

Both types of WTP cells featured a coaxial reentrant thermowell suitable for immersion of a long-stem SPRT. The thermowell depth was sufficient to allow adequate immersion for all

varieties of SPRTs with a typical full depth of 27 cm between the bottom of the well and the free surface of the water when held in a vertically aligned position. As is the case for all immersion-type fixed point cells, a correction is needed to account for the immersion depth of the thermometer. This correction adjusts for the increased pressure at the sensing element position at a depth relative to the free surface where the pressure is known. The so-called ‘hydrostatic head correction’ is given by

$$\Delta T_h = \frac{dT}{dp} \cdot \rho g \Delta h, \quad (1)$$

where dT/dp is the inverse slope of the melting line of the p - T phase diagram (-7.5×10^{-8} K/Pa), ρ is the density of the liquid water head, g is the acceleration due to gravity and Δh is the hydrostatic head between the sensing element and the water free surface. The head correction coefficient is readily determined as $\Delta T/\Delta h = -0.735$ mK/m and a typical associated shift in temperature is -0.180 mK at the position of the SPRT sensing element near the bottom of the well (an effective head depth of 245 mm). In practice this shift is always close to -0.18 mK in most cells (i.e. 0.18 mK *colder* near the bottom of the well) and a correction need not be applied when comparing like cells using like SPRTs, such that all combinations yield similar shifts in temperature as locally equilibrated with by the SPRT sensing element. This is the case for all of the NIST comparison data reported in this study (i.e. the resistance values are uncorrected for the hydrostatic head shifts). An uncertainty of the hydrostatic head shift temperature of 2 % (i.e. ~ 0.004 mK) accounts for any departures from this assumption (see section 5.1.1).

It should be recognized that only $\frac{3}{4}$ of the known shift of 0.010 °C between the WTP (273.16 K) and the Ice Melting Point (IMP, 273.15 K) is due to the slope of the melting line for the solid-liquid equilibrium of the chemically pure phases. The remaining -0.0025 °C shift is due to the freezing point depression produced by dissolved air as the mixture equilibrates with air at 101.325 kPa pressure. The two separate contributions lead to the 0.01 °C difference between the triple point and the air-saturated normal melting point and have been confirmed via both thermodynamic calculations and contemporary experiments. [9]

The commercial production of WTP cells has advanced to a point where high quality and low defect rates are achievable for any of several manufacturers worldwide. Costs in 2023 are typically between 3 to 5 thousand dollars US each depending on the glass and model types. While they are highly stable and indispensable in temperature metrology, their fragile nature inevitably leads to occasional accidents and breakages. This almost always results in the irrecoverable loss of a cell but replacements are continuously being produced and put into service. The breakage under transport is perhaps the most prevalent accident, but accidental breakage can also occur in less predictable scenarios under normal laboratory use. This situation leads to some unique challenges when large numbers of cells are being shipped and collected for the purposes of an international comparison. The circumstances surrounding the NIST participation and subsequent withdrawal from the K7.2021 comparison illustrates the extent of these challenges.

2.2. The water isotopic composition and revised definitions

By the late 1990s two problems were recognized regarding the use of borosilicate WTP cells in their contemporary production across all sources throughout the world. The first problem concerned the apparent aging of WTP cells when older cells were compared with newer cells of the same type and or source [10]. The WTP realizations in the oldest cells were often, but not always, colder than those of newer cells. It was hypothesized that the metallic ions of sodium and boron present in borosilicate glasses could slowly dissolve into the water and lower the freezing point temperature [11]. The effects were dependent on the methods of cleaning for the glass surfaces employed during preparation of the cells and also the temperature at which the cells were stored over time. Eventually cell production expanded to include the use of pure fused silicate glass where the higher purity material led to a much lower dissolution rate compared to borosilicate glass and those silica-glass cells indeed exhibited a greater degree of stability over time [12].

The second problem that emerged during the 1990s concerned the isotopic composition of the water. It had long been recognized that there was a slight difference between the melting point of waters derived from continental surface water versus that of ocean waters. This difference originated in isotopic fractionation that occurred during the water cycle that fed the continents with fresh water precipitation having a slightly lower fraction of heavier isotopes, deuterium ($^2\text{H}\equiv\text{D}$) and oxygen-18 (^{18}O) [13]. Furthermore, the cell-production distillation process itself could impart fractionation that would vary according to the exact method employed and the degree to which a distillation for a given cell was run to completion or if a substantial fraction of undistilled water was left behind [14]. The working definition of the WTP from the text of the IPTS-68 [15] included a footnote that read: “The water used should have the isotopic composition of ocean water...”. However, there was no official or otherwise generally agreed equation which could be used to affect corrections when using water that deviated from ocean water or any specification for an unambiguous reference composition. The text of the ITS-90 was even more vague [1], specifying only that the water is “...of natural isotopic composition”. Furthermore, the original SI definition of the kelvin was from 1954 and made no mention of the water’s isotopic composition.

The customary variables for the quantifying the isotopic content of water are defined as dimensionless relative variations with respect to that of Vienna Standard Mean Ocean Water (V-SMOW) for a given isotope. These are notated as δD for the deuterium content, $\delta^{18}\text{O}$ for the ^{18}O content and $\delta^{17}\text{O}$ for the ^{17}O content. The range of values found for terrestrial natural water is approximately $-0.250 \leq \delta\text{D} \leq +25$ and $-32 \leq \delta^{18}\text{O} \leq +4$ and these variations are highly correlated. This correlation is known as the Global Meteoric Water Line (GMWL) [13].

It should be mentioned that isotopic fractionation during the distillation of the water in the preparation process was likely something that always had occurred but remained obscured for decades. This was due to the fact that isotopically ‘light’ water would lower the realization temperature, which was the same sign for the shifts due to both dissolved ions and dissolved

air. Thus ‘cold’ WTP cells that had been isotopically fractionated, but were otherwise perfect, were sometimes mistaken for ‘bad’ cells with some presumed excessive amount of dissolved air.

This situation with ambiguous or otherwise unknown isotopic fractionation led to a redefinition of the unit kelvin by the CIPM in 2005 [16]. Around this same time, the CCT added supplemental information concerning the WTP and isotopic corrections to the Technical Annex for the Mise-en-pratique for the realization of the kelvin [17]. Corrections could then be made when the actual isotopic content was known via an equation,

$$T_{\text{meas}} = T_{90}(\text{TPW}) + A(\text{D}) \cdot \delta\text{D} + A(^{18}\text{O}) \cdot \delta^{18}\text{O}, \quad (2)$$

where $T_{90}(\text{TPW})=273.1600(1)$ and the coefficients are $A(\text{D})=673(4)$ and $A(^{18}\text{O})=630(10)$. These coefficients are well known from detailed studies carried out at the Van Swinden Laboratory (VSL, the National Metrology Institute of the Netherlands) [18] and are in agreement with calculations using other literature data [19]. Water samples could be taken from batch distillations or from portions of actual cells in production prior to the final sealing of the cells. Those water samples are readily analyzed for isotopes of hydrogen and oxygen through well-established analytical chemistry methods commonly employed in environmental geochemistry [13].

In 2019 the CIPM redefined the kelvin in terms of the Boltzmann constant [20], ending the special status of the WTP that had been in place since 1954. Nonetheless, the WTP still maintains a critical role in the ITS-90 and remains the most important fixed point for the dissemination of the scale via SPRTs. The WTP temperature now carries an additional thermodynamic uncertainty to its assigned temperature that was essentially transferred from that of the Boltzmann constant such that $T_{\text{wtp}} = 273.1600(1)$ K.

2.3. The use of water triple point cells at NBS/NIST

The NBS/NIST has used commercially-sourced WTP cells since the late 1950s when the Wheaton MD facility began producing cells. These ‘Jarrett’ cells were always made from borosilicate glass and the water derived from continental surface water originating from the Potomac River. The NIST SPRT calibration laboratory had historically maintained a large stock of type A Jarrett cells for the purposes of temperature scale dissemination during the years leading up to the closing of the Wheaton MD commercial facility. For the purposes of realization, these cells were historically maintained in ice-water (‘slush’) baths up until the late 1980s. Since the advent of the ITS-90, NIST WTP cells have been maintained in specialized Peltier-cooled liquid baths holding up to four cells. The four-cell capacity of the maintenance bath allowed for the precise comparison of cells as well as the normal calibration workload for SPRTs. A special internal WTP comparison study took place in 1997 where the fine-scale equilibration associated with variable stress relaxation effects, as induced by employing different freezing methods, was demonstrated [22]. That study employed four of the Jarrett

type A cells from the NIST stock of WTP cells in place within the SPRT Calibration Laboratory at that time.

Starting in the mid-1990s, other domestic commercial sources of high-quality cells became available and NIST began to purchase and put those newer type A cells into service in the NIST SPRT calibration laboratory. This mix of stock type A cells from the old Wheaton facility and the newer production elsewhere were employed by NIST for the purposes of ITS-90 realization [23] and the CCT K7 WTP comparison [2] that began in 2002.

Starting in 2006, the NIST Low Temperature Calibration Facility (LTCF) began maintaining a separate and independent set of WTP cells for scale maintenance purposes specific to capsule-type SPRTs and other low-temperature capsule-type thermometers. These cells were of the type B and type C designs and maintained in a small refrigerated forced-convection-water/ethanol bath having a capacity for two cells [24].

At the time of the CCT K7 in 2002, isotopic analysis of the water was not generally available as a service for buyers of commercial WTP cells. Consequently, NIST did not have isotope composition data available for the CCT K7 comparison. This situation gradually changed over the next few years as the commercial cell manufacturers began to alter their procedures for preparation of WTP cells. A common method would be to combine the distillation steps, which tended to deplete (i.e. lighten) the water of the heavier isotopes, with a vacuum degassing step, which tended to enrich (make heavier) the water of heavier isotopes. In some cases, manufactures may also be adding isotopically enriched water to the batch process water. This combination allowed an empirical process to be developed in which the final composition of the water contained in each cell would be close to that of the V-SMOW reference composition. The manufacturers then started to provide certificates along with each cell with the results of isotopic measurements stating either the tolerance range or actual deviations of the ^2H , ^{18}O and ^{17}O isotopic content relative to that of VSMOW [25].

The commercial production of WTP cells made from fused-silica (or fused-quartz) glass also was phased in over the years following the K7 comparison. Since about 2004, these higher quality cells have been generally available from at least two commercial sources. These fused-silica glass cells are produced with essentially the same designs of the original types A and B cells, with some small variations in the inner and outer diameters. NIST has subsequently built up and maintained a stock of fused-silica-glass cells with known isotopic content [26] and these have been in regular service since about 2007 [26][27].

The experience gained from the K7 WTP comparison and by many NMIs using fused-silica WTP cells in the following decade greatly improved the methodologies and materials employed in the realization of the WTP. Once the exhaustive VSL isotope study [18] was completed in 2015, the CCT compiled a new guide on the WTP realization that summarized the most significant findings and best practices, most recently updated in 2018 [28].

3. The CCT international comparisons for the water triple point

A total of three international comparisons of WTP cells have taken place within the last 25 years.

3.1. BIPM international comparison of triple point of water cells (1994-1995)

The first of these comparisons was organized and piloted by the BIPM and was conducted with 12 participating MNIs from 1994 to 1995 [21]. The Pilot chose a set of ten WTP cells of contemporary origin (both commercial and NMI laboratory fabricated) and distributed six of those cells to six of the participating NMIs for comparison to the NMI's reference cells. Two of these were Jarrett cells as directly sourced from the Wheaton MD facility while the other eight cells were made in the laboratories of five NMIs. The BIPM performed measurements of these 'traveling cells' in comparison to a set of four cells designated as the 'reference set'. In addition, the BIPM made comparisons of a number of other cells sent in from other participating NMIs relative to the reference set. NIST participated in the comparison as one of the six NMIs performing measurements relative to an in-house reference cell. This comparison was sanctioned by the CCT, but did not have the status of a 'Key' comparison due to the fact that it was initiated prior to the enactment of the Mutual Recognition Arrangement (MRA) in 1999.

The results of this first BIPM comparison indicated a level of agreement between the cells that was slightly worse than what was achieved in 1982 at NBS [7] using only the Jarrett cells. Most of this dispersion in the realization temperatures could be attributed to some degree of instability in two of the traveling cells. The distribution of cell temperatures in the original ten WTP cells ranged from $\sim +0.11$ mK to -0.19 mK with respect to the reference cell's temperature. In contrast, the two Jarrett cells agreed with each other to within less than ~ 0.01 mK and their realization temperatures were both $+0.11$ mK relative to the BIPM reference cell. Measurements made at NIST combined with those at the BIPM indicated that the NIST reference cell (identified as 'NIST-4') was about $+0.09(4)$ mK hotter than the BIPM reference cell. All of the cells were made from borosilicate glass and no cell age information was made available.

3.2. CCT-K7 (2002-2004)

The BIPM was again the pilot laboratory for the CCT-K7 international comparison.[3] The technical protocol for the K7 comparison was finalized in June 2002 with a total of 21 participants including the BIPM and NIST. Prior to the start of the comparison, one of the two principal investigators at the BIPM was detailed to the NIST SPRT calibration laboratory for special training with the NIST scientific staff.

The K7 technical protocol was highly detailed and specified a set of rigorous experimental procedures designed to produce the highest level of reproducibility and reliability for the results. The K7 protocol established the role of the 'transfer cells', as submitted by the

participants for use in the comparison, and that of the ‘national standard’ cell(s) representing how the WTP is realized within each of the participant’s laboratories. The objectives of the K7 were to a.) quantify differences between a set of transfer cells and b.) establish values for the differences and uncertainties between the transfer cells and the national reference cells(s) from each participating laboratory.

The K7 results were compiled from comparisons of 21 transfer cells against two BIPM reference cells. The bulk of the data were obtained over a seven-month period over which two separate ice mantles were constructed for each of the transfer cells, over a time frame which was generally within 30 days. The ice mantles were constructed using the widely accepted practice sometimes referred to as the ‘dry-ice method’ or otherwise known as the *Crushed solid-CO₂ method* [22].

NIST submitted a commercial WTP cell, serial number 1040 (manufactured in 1999). Most if not all of the transfer cells were probably made from borosilicate glasses, but in general the glass types used for the various transfer cells were not specified in the K7 report. Most of the transfer cells submitted for the K7 had unknown isotopic compositions. Although six of the 21 participating NMIs had isotopic analyses pertaining to their transfer cells, the water used in the NIST transfer cell did not have an isotopic analysis.

A Key Comparison Reference Value (KCRV) was adopted for the purposes of the CCT-K7 comparison. Here we quote from the final report regarding the KCRV:

“...the KCRV is based on the mean value of the results from all of the participants, including some laboratories who made corrections for the influence of chemical impurities and isotopic composition, and some who did not. The uncertainty of the KCRV is taken to be the standard deviation of the mean of the data set. Because the distribution of the pooled data is multimodal, care should be taken when using this quantity for calculating confidence intervals.”

The uncertainty in the K7 KCRV was as such calculated to be 11 μK , but the standard deviation for the entire distribution of 21 temperature difference values (BIPM + 20 NMIs) was $(21)^{1/2} = 4.58$ times larger, or $\approx 50 \mu\text{K}$. The results for the NIST transfer cell were $\Delta T = T_{\text{NIST}} - T_{\text{KCRV}} = -62(34) \mu\text{K}$ relative to the KCRV. However, the difference with respect to the NRC transfer cell, which had an isotopic analysis and was corrected to the VSMOW composition, was $\Delta T = T_{\text{NIST}} - T_{\text{NRC}} = -124(43) \mu\text{K}$.

Strouse and Zhao [26] have described the steps taken at NIST post K7 to study both dissolution of impurities and isotopic variations found in commercial borosilicate glass WTP cells. Based on ex post facto analysis of water samples taken from other WTP cells during the time of manufacture of the NIST transfer cell 1040, it was inferred that the water in this cell was probably isotopically depleted such that it would have been 80 μK low with respect to a VSMOW composition WTP cell [25]. Comparison data taken at NIST between 2005 and 2006 confirmed that both the NIST transfer cell 1040 and the NIST reference cell 1041 had realization temperatures that were 72 μK below that of various new cells with VSMOW composition [26].

Despite this ex post facto correction, some unresolved discrepancies remain in the K7 comparison data. No follow up work could be conducted past 2007, however, due to a series of unusual accidents within the SPRT calibration laboratory at NIST resulting in breakages of the K7 transfer and reference cells in 2008.

3.3. CCT-K7.2021 (2021-2022)

The CCT-K7.2021 comparison was organized and piloted by the National Research Council in Ottawa Canada.[2] The objectives of the K7.2021 were to : a.) conduct “*a comparison....of the participant national realizations of the TPW temperature*”; b.) produce a “*direct comparison of TPW cells of the highest quality*”; and c.) provide “*linkage to the previous key comparison CCT-K7,*”. The original 19 NMI participants had agreed to the protocol by December 2020 and that was approved by the CCT Working Group on Key Comparisons in January 2021. Extensive preparation activities took place at the NRC prior to the comparison [29]. Measurement activities ran from April 2021 to September 2022, beginning with initial measurements at the participants’ laboratories.

The protocol for the K7.2021 was similar to that of the original K7 comparison, again establishing degrees of equivalence between the participating NMI’s ‘National Reference Cells’ via their respective transfer cells as sent to the NRC for the comparison measurements. However, in the case of the K7.2021, more detailed information was requested from the participants than before. In particular, information was requested concerning the chemical impurities and isotopic content of the National Reference Cell.

NIST was among the original 19 participants in the K7.2021 and submitted a transfer WTP cell to the NRC for the purposes of the comparison. Unfortunately, this original transfer cell suffered a breakage while at the NRC in November of 2021 prior to any comparison measurements. NIST then sent a replacement transfer cell (serial number ID ‘1454Q’) in December of 2021 which was received at the NRC and a full set of comparison data was obtained using this replacement cell. That replacement cell was later hand carried back to NIST on May 31 of 2022 and NIST took custody of the cell in preparation for a final set of comparison measurements to be conducted at NIST. Once returned to NIST, this cell then suffered an unrecoverable breakage on June 1, precluding any further use of that cell for the CCT-K7.2021. NIST then withdrew from the K7.2021. Two other NMIs also withdrew for similar reasons and a third NMI withdrew for other reasons, leaving a net of 15 NMIs participating in the comparison through to the completion.

Since the breakage of the NIST replacement transfer cell occurred after the NRC had completed the comparison measurements on that cell, the comparison data linking the NIST cell to the results of the comparison and to the KCRV exist. The NRC made comparisons of the transfer cells that were divided into four batch runs (I, II, III, and IV) of five to six cells each. The final report for the K7.2021 contains a table for the Batch IV comparison of transfer and reference cells conducted from 31-Jan to 8-Mar 2022. The NIST transfer cell 1454Q was included in this

comparison batch and the results of those measurements using that cell are included in Table 4.6. of the final report [2]. The results do not appear in the accompanying plots and following tables of those data, so we have reproduced a plot of those data here with the NIST transfer cell included, as shown in Figure 2 and in Tables 1 and 2 below.

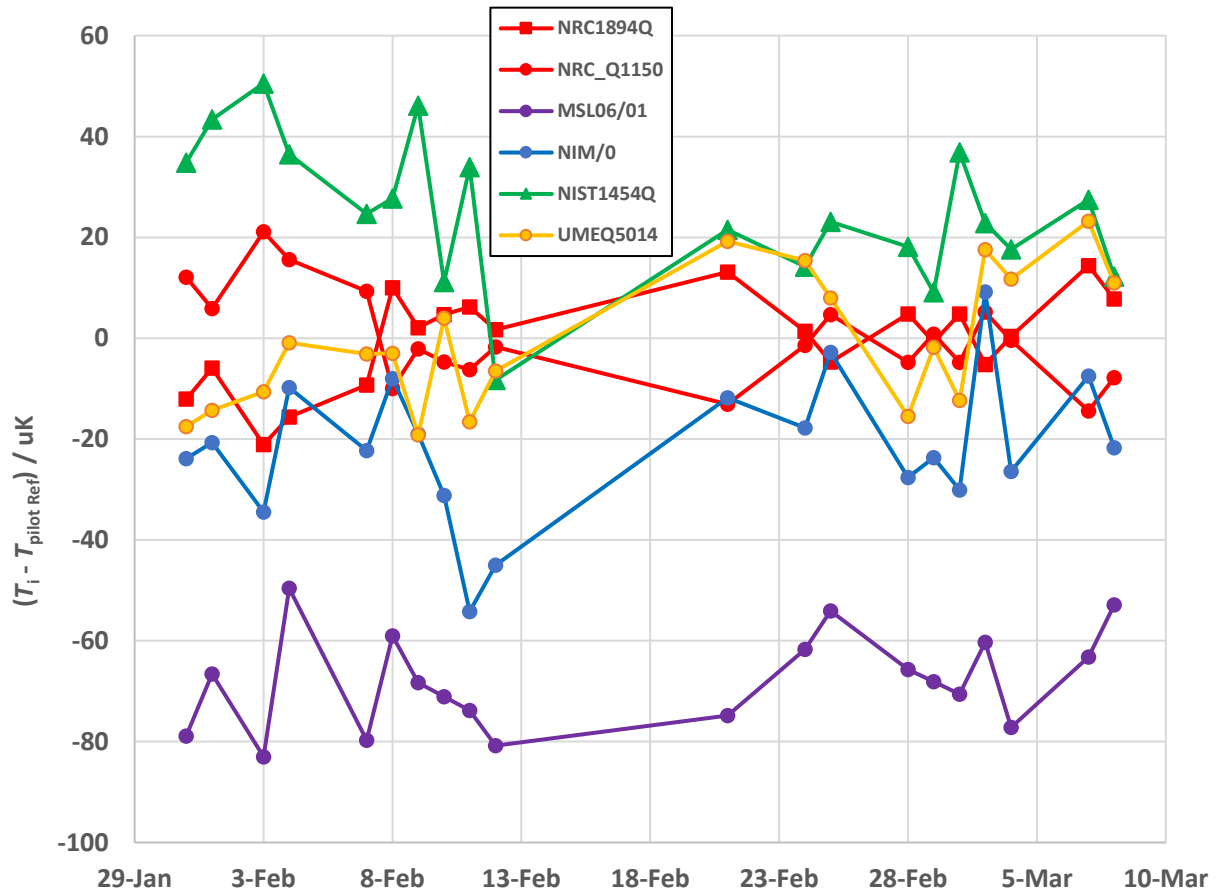


Figure 2. A reproduction of data from the CCT-K7.2021 comparison batch IV during February and March of 2022, including data from the NIST replacement transfer cell 1454Q. Data are expressed in terms of temperature differences with respect to the NRC reference cells. Data from two separate ice mantles are shown, with the second mantle series starting on Feb 21.

The NRC comparison data from the K7.2021 allows a direct calculation of the WTP realization temperature from 1454Q relative to that of the NRC reference cells ('Pilot Reference'), and in turn to the KCRV for that comparison. The results shown in Table 2 indicate that $T_{NIST}^{Xfer} - T_{Pilot Ref} = 25(9) \mu\text{K}$ for both ice mantles, which is slightly more positive than any other cell included in the K7.2021 comparison. Some of that positive deviation can be attributed to the unusual distribution of heavy isotopes of hydrogen and oxygen in the NIST transfer cell, 1454Q (see section 5.2). The statistical uncertainty is $14 \mu\text{K}$ from the standard deviation of all 20 observations for that cell. A combined standard uncertainty of $13 \mu\text{K}$ is derived for pair comparisons by the pilot laboratory. There is a reduction in this uncertainty by a factor of $\sqrt{2}$

(i.e. 9.3 μK) when a given difference result is computed relative to the Pilot Reference temperature since this was defined as an average between the temperatures from 2 NRC reference cells. Hence, we use the value of $T_{NIST}^{\text{Xfer}} - T_{\text{Pilot Ref}} = 25(9) \mu\text{K}$ from the NRC data.

A KCRV was computed for the K7.2021 comparison via an adaptive weighted average method. The result was $T_{\text{KCRV}} - T_{\text{Pilot Ref}} = 4.7(7.2) \mu\text{K}$ [2].

Table 1 A partial reproduction of Table 4.6 ‘Results of Batch IV’ from the K7.2021 Report including resistance data for the NIST1454Q.[2]

NRC1894Q	NRCQ1150	MSL06/01	NIM/0	NIST1454Q	UMEQ5014
Ohms	Ohms	Ohms	Ohms	Ohms	Ohms
25.56510923	25.56511169	25.56510242	25.56510802	25.56511401	25.56510868
25.56511038	25.56511159	25.5651042	25.56510887	25.56511541	25.56510953
25.56510875	25.56511307	25.56510245	25.5651074	25.56511606	25.56510983
25.56510935	25.56511254	25.5651059	25.56510995	25.56511466	25.56511085
25.56510863	25.56511052	25.56510145	25.5651073	25.56511209	25.56510925
25.5651106	25.56510857	25.56510357	25.56510877	25.56511241	25.56510928
25.56511123	25.56511079	25.56510405	25.56510907	25.56511571	25.56510905
25.5651102	25.56510924	25.56510247	25.56510655	25.56511086	25.56511013
25.56511133	25.56511007	25.56510317	25.56510517	25.56511416	25.565109
25.5651106	25.56511027	25.5651022	25.56510585	25.56510959	25.56510978
25.56511178	25.56510912	25.56510282	25.56510925	25.56511264	25.5651124
25.56511	25.56510972	25.56510357	25.56510805	25.56511131	25.56511143
25.56510955	25.56511052	25.56510452	25.56510975	25.56511239	25.56511085
25.56511045	25.56510947	25.56510327	25.56510715	25.56511181	25.56510838
25.56511083	25.56511099	25.56510397	25.5651085	25.56511184	25.56511073
25.56511088	25.56510989	25.56510319	25.56510732	25.56511414	25.56510913
25.5651083	25.56510937	25.56510269	25.56510977	25.56511116	25.56511063
25.56510905	25.56510897	25.56510114	25.56510632	25.56511081	25.5651102
25.56510873	25.56510579	25.56510082	25.5651065	25.56511006	25.56510963
25.5651091	25.56510752	25.56510292	25.5651061	25.56510956	25.56510943

Table 2 A partial reproduction of Table 4.6 ‘Results of Batch IV’ in the K7.2021 Report including temperature difference data for the NIST1454Q.[2]

Cell ID:	NRC1894Q	NRC_Q1150	MSL06/01	NIM/0	NIST1454Q	UMEQ5014
	[μ K]	[μ K]	[μ K]	[μ K]	[μ K]	[μ K]
M1-1	-12.1	12.1	-78.9	-23.9	34.8	-17.5
M1-2	-5.9	5.9	-66.6	-20.7	43.4	-14.3
M1-3	-21.1	21.1	-83	-34.5	50.5	-10.6
M1-4	-15.6	15.6	-49.6	-9.8	36.5	-0.9
M1-5	-9.3	9.3	-79.7	-22.3	24.7	-3.1
M1-6	10	-10	-59	-8	27.7	-3
M1-7	2.1	-2.1	-68.3	-19	46.1	-19.2
M1-8	4.7	-4.7	-71.1	-31.2	11.2	4
M1-9	6.2	-6.2	-73.8	-54.2	33.9	-16.6
M1-10	1.7	-1.7	-80.8	-45	-8.3	-6.5
M2-1	13.1	-13.1	-74.8	-11.8	21.5	19.2
M2-2	1.4	-1.4	-61.7	-17.8	14.2	15.4
M2-3	-4.7	4.7	-54.1	-2.8	23.1	8
M2-4	4.8	-4.8	-65.7	-27.6	18.2	-15.5
M2-5	-0.8	0.8	-68.1	-23.7	9.1	-1.8
M2-6	4.8	-4.8	-70.6	-30.1	36.8	-12.3
M2-7	-5.2	5.2	-60.3	9.2	22.8	17.6
M2-8	0.4	-0.4	-77.2	-26.4	17.7	11.7
M2-9	14.4	-14.4	-63.2	-7.5	27.5	23.2
M2-10	7.8	-7.8	-52.9	-21.7	12.3	11
Average M1	-3.9	3.9	-71.1	-26.9	30.1	-8.8
Average M2	3.6	-3.6	-64.9	-16.0	20.3	7.7
Average M1+M2	-0.2	0.2	-68.0	-21.4	25.2	-0.6

4. Experimental systems and results at NIST

In this section we describe the WTP cells, the measurements and the results from the LTCF to compare the two NIST WTP cells, 1454Q and Q1034.

4.1. Comparison of water triple point cells in the NIST LTCF

Capsule-type SPRTs have been used to maintain the ITS-90 below 84 K within the NIST LTCF since 1994 [24]. This activity involved periodic measurements of the WTP for those capsule SPRTs. This was accomplished using the WTP cells maintained in the NIST SPRT Calibration Laboratory until 2006, when the installation of new cells and a maintenance bath within the LTCF allowed for independent WTP realizations for those purposes.

Occasional two-cell comparisons have taken place within the LTCF for the purposes of qualifying new WTP cells as they were acquired and put into service. As a result, there are comparison data on a number of different WTP cells in use there since 2006, including both borosilicate and fused-silica-glass types. These data are derived from multiple ice mantles with multiple capsule SPRTs spanning multiple years. For the purposes of this report, we are focusing on just two fused-silica-glass WTP cells and their use within the LTCF during a 5 year period. These are identified as serial number Q1034 (Type C), purchased in 2013 and serial number 1454Q (Type B), purchased in 2015.

The cell Q1034 has served as the NIST reference cell for the purposes of capsule SPRT calibrations and ITS-90 scale maintenance within the NIST LTCF since 2015. The cell 1454Q had served in a similar capacity on an occasional basis since 2016 and was selected as a replacement transfer cell for the purposes of K7.2021 in December of 2021 (see section 3.3). No special preparation or planning for this new role for 1454Q had occurred since this was essentially an immediate and unanticipated need. While the cell 1454Q no longer exists, the cell Q1034 is still in service at this writing. Table 3 provides some essential characteristics and information concerning these cells, providing essentially the same information as do the Tables 3.1 and 3.2 from the K7.2021 report [2].

Table 3 Summary information for the WTP cells used by NIST for this study.

Serial no.	Role	Source	Model	Year	Isotopic Data	Isotopic Correction	Chemical Data
1454Q	Transfer	Isotech	B13-65-270	2015	Yes	No	No
Q1034	Reference	Fluke	5901C-Q	2013	Yes	Yes	No

We restrict the WTP data to the five-year time period from 2017 to 2022 which includes some overlap with the performance period of the CCT K7.2021. However, only some of SPRTs in use within the LTCF had a history of use with both of these WTP cells during this period of time. When this selection criterion is applied, the qualified measurement data are taken from seven capsule-type SPRTs and one long-stem type SPRT, with six separate ice mantles for Q1034 and three separate mantles for 1454Q. The associated sequence of dates for the initiation of these

ice mantles are shown together with unique labels that identify the specific WTP mantles in Table 4.

It is noteworthy that a gap of approximately 2 years is evident in Table 4 over which no data was available. This gap coincides with the shutdown of the NIST laboratory facilities starting in March of 2020 due to the Covid-19 pandemic and the subsequent restrictions on activities that were in place after the facilities were reopened in September 2020. During the 6 month shutdown, all equipment was powered off and environmental controls were not engaged in most of the Gaithersburg campus buildings, leading to unknown storage temperatures for the WTP cells. During the restart of laboratory activities in late 2020, equipment failure occurred in the LTCF and the refrigerated stirred-water/ethanol bath was unavailable until August of 2021 (Mantles 21B). Consequently, the mantles identified as 21A in Table 4 were maintained in a different stirred-water/ethanol bath having less-optimized characteristics.

Table 4 The usage history of the WTP cells Q1034 and 1454Q in the NIST LTCF from 2017 through 2022. The dates shown are those associated with the initiation of various ice mantles which are given labels as shown in the two cells' columns. Also shown are other dates associated with each cell's history (see text).

Date	Q1034	1454Q
30-Mar-2017	17A	
18-May2017		17B
10-Jul-2018	18A	
11-Mar-2019	19A	
March-20	Covid-19 Facility Shutdown Starts	
September-20	Covid-19 Facility Shutdown Ends	
7-Apr-2021	21A-1	21A-2
11-Aug-2021	21B-1	21B-2
18-Nov-2021		Removed from service
Dec-21		Shipped to NRC
1/31/2022		NRC M1
2/21/2022		NRC M2
3/15/2022	22A	
5/31/2022		Returned to NIST
6/1/2022		Broken

The data are derived from cell comparisons made in the course of laboratory quality checks and other activities specific to scale maintenance, stability checks, research, and calibrations. Consequently, the data are an admixture of deliberate comparisons of the two cells taken over a short time interval (e.g. one or two days) and other less direct and essentially coincidental comparisons derived from measurements over longer time intervals (i.e. up to 3 years in some cases). An allowance for potential SPRT instability is included in the uncertainties (see section 5.1 below) to account for this non-ideal situation. However, all of the SPRTs included here are NIST reference and check standard SPRTs with histories of usage sufficient to convey confidence in their stability. Table 5 shows which SPRT data are available for each of the different ice mantles included in this study.

Table 5 Information mapping the SPRTs and cell mantles used as the basis for the comparison results.

s/n	17A	17B	18A	19A	21A-1	21A-2	21B-1	21B-2	22A
1774092	F	F	F			F			F
1774096	F	D1	F			F			
1842385	F		F			F			F
56860103	F	F	F	D1	F, D2	D2	F	F	
RS163-01			F			F			
RS163-04			F			F			
56811538§							F	F	
162D3363			F	D1	D2	D2			

Letter designations F & D refer to experimental set ups, (see text, section 4.3). Blue color indicates cell Q1034 and red indicates cell 1454Q.

§ A long-stem thermometer

4.2. WTP cell Comparisons for the Boltzmann constant determination

The results of a small fraction of the data selected for this report have been previously published for the purposes of the 2017 CODATA determination of the Boltzmann constant, k_B [30]. This was associated with a specific set of WTP comparisons occurring at NIST for a determination of k_B [31]. Those results appear in Table 1 of reference [31] and include a direct comparison of the cells Q1034 and 1454Q from May 16 to 19, 2017. These data were derived from measurements of SPRT 1774092 and the WTP realizations labeled 17A and 17B in Table 4 of the previous section. Those data yielded good agreement between the cells with an observed difference of $-0.024(23)$ mK. This will be discussed in further detail in the Discussion section 5.3 below.

4.3. Experimental procedures

The seven capsule-type SPRTs were adapted for immersion use via one of two sizes of borosilicate tubing adapters. One size accommodates certain models of low-profile capsules using tubing of Inner Diameter/Outer Diameter (ID/OD) of 5.8 mm / 7.6 mm which have been used in the NIST SRM 1750 capsules SPRTs [32]. The other adapter tubing ID/OD size is 9.0 mm / 11.0 mm for accommodating traditional capsule-type models having bulbous glass headers. Aluminum bushings are used in both styles of tubing adapters. In the case of the 5.8 mm / 7.6 mm adapters, the bushing is ‘wet’, inserted into the WTP cells’ thermowell as would normally be done for a long-stem SPRT. In the case of the 9.0 mm / 11.0 mm adapters, the bushing is ‘dry’, and inserted between the capsule sheath and the adapter tube’s ID. Examples of these adapter probes are shown in Figure 2. Additional details are available in section 4.2.1 of reference [24].

The ice mantles were constructed using the same crushed solid- CO_2 method [22] as was used for the K7 and K7.2021 comparisons. The annealing period prior to use was as short as 48 hours, a departure from the K7 protocols of 7 days. The K7.2021 protocol specified at least 10 independent measurements for the each of 2 ice mantles, applicable to both the transfer cells and the reference cells. The available data for this report was limited to a total of 16 independent measurements over a total of 3 ice mantles for the transfer cell and a total of 39

independent measurements over 6 ice mantles for the reference cell. The detailed distributions of measurements for all of the ice mantles are shown in Table 6. Most other procedures were similar to those specified in the K7 protocols, and Table 7 lists the most significant procedural protocols for this work in comparison to those specified in the K7 protocols.

Table 6 The measurement distribution for the SPRTs and Ice Mantles reported here.

s/n	17A	17B	18A	19A	21A-1	21A-2	21B-1	21B-2	22A
1774092	2	3	2			1			1
1774096	4	1	2			1			
1842385	5		1			2			1
56860103	1	2	1	2	2	1	1	1	
RS163-01			2			1			
RS163-04			2			1			
568115385							1	1	
162D3363			5	3	1	1			
Totals	12	6	15	5	3	8	2	2	2

Table 7. Procedures and data specified in the K7.2021 protocol and as provided in this work.

Procedure	K7.2021 Protocols	This Report
Transfer Cell Mantles	Two minimum	Three
Mantle Annealing time	> 7 days	> 2 days
Transfer Cell Measurements / Mantle	≥ 10	See Table 6
Reference Cell measurements / Mantle	≥ 10	See Table 6
Inner Melt Induction	Before each measurement	Before each measurement
Use of Bushings	Optional	Yes (see text)
Immersion Profile	Required Data	Appendix A
Post-Pilot Comparison at NIST	Required Data	Not Possible
Self-heating corrections	Required	Series F and D1 (see 4.4)
Hydrostatic Head Corrections	As needed	Not applied (see 5.1.1)
Isotopic Correction	Optional	See section 5.1.2
Isotopic Certificate of Analysis	Required Data	Appendix B
Uncertainty Budget	Required Data	Section 5.2



Figure 3. Examples of capsule-type SPRTs as adapted into glass tubing for immersion use in WTP cells. A.) 9.0 mm ID / 11.0 mm OD probe for accommodating traditional capsule-type models. B.) 5.8 mm ID / 7.6 mm OD probe for accommodating low-profile capsule models. C.) traditional-style capsule SPRT with Pt sheath intact. D.) traditional-style capsule SPRT with Pt sheath removed.

4.4. NIST WTP Data

The data were obtained by measurement of the SPRTs with two different resistance bridge instruments. These data were primarily the product of routine quality checks and incidental research activities within the LTCF, and only a small fraction of these data were produced with the deliberate intent of comparing the two WTP cells. The target standard uncertainty for most of these measurements was 0.05 mK. We describe below the data from these two instruments as two separate series of experiments, however, it is possible to combine most of the resistance data and all of the temperature data when expressed as temperature differences between the two WTP cells.

4.4.1. F Series

Most of the measurements, designated as the 'F' in Table 5, were performed using an auto-balancing inductive-voltage-divider (IVD) ratio bridge using 30 Hz sine wave excitation. This bridge was referenced to a calibrated 100 Ω standard resistor held at 25.0(1) $^{\circ}\text{C}$. Readings were obtained in three sets of 36 at 1 mA, 2 mA, and 1 mA excitation currents. The zero-power corrected resistance values were computed along with the extrapolated uncertainty based on the standard deviations observed at each of the finite current data sets of 36 readings. This resulted in a sparse collection of TPW data over the five year collection interval. An example of the zero-power corrected resistance data for one of the SPRTs (1774092) is shown in Figure 4.

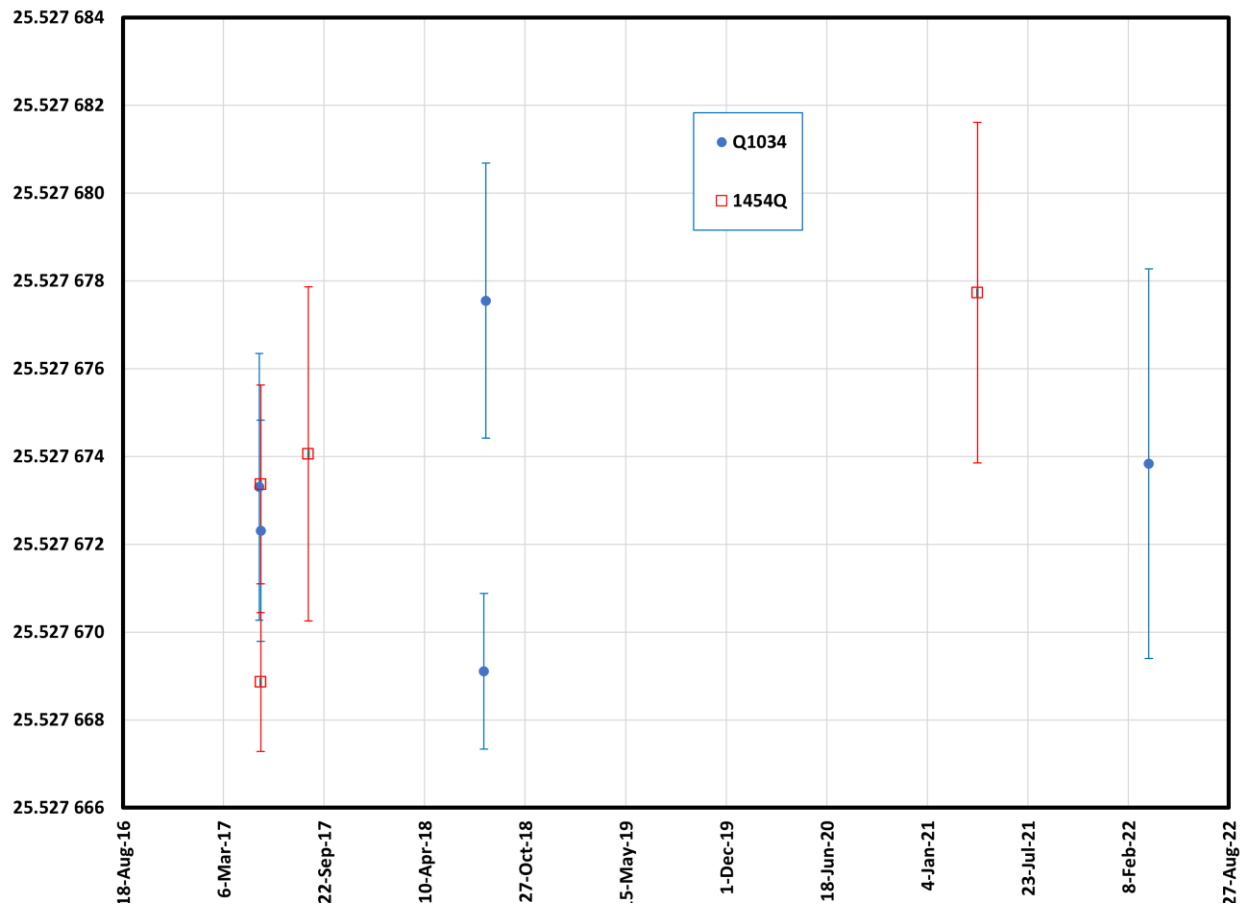


Figure 4 WTP zero-power resistance data from capsule SPRT 1774092

A calibrated SPRT was inserted into the central thermowell of the standard 100 Ω reference resistor to record air bath temperature. The recorded resistance ratios from the F series data were ex post facto corrected for variations in the air bath temperature affecting the value of the reference resistor, having a temperature coefficient of resistance of $-0.4 \mu\Omega/\Omega/^{\circ}\text{C}$ at 25 $^{\circ}\text{C}$. However, these local temperature readings were not available during the 2017 (17A and 17B) F-series measurements. This results in a slightly higher uncertainty in the bridge measurements for those data series.

4.4.2. D Series

A second resistance bridge was also used for a smaller subset of the experiments, as shown as D1 and D2 in Table 5. In this case the data were obtained using a digital substitution bridge (DSB) operating with a 5 Hz square wave excitation. This bridge was referenced to a calibrated 25 Ω standard resistor held at 27.7(1) °C. This bridge was used in two different ways, identified as series D1 and series D2. In the first method, D1, the DSB made measurements in three sets of 30 readings at 1 mA, 2 mA, and 1 mA excitation currents, just as was done in the F-series measurements. Those results allow extrapolation to zero power in the usual way.

In the second method, designated D2, as performed on one specific date (9-Apr-2021), two SPRTs were read simultaneously as two separate time series at 1 mA in each of the two TPW cells shown in Table 1. Then after equilibrating and recording the data, the two SPRTs were interchanged into the other cells and again allowed to equilibrate while continuously recording the time series for both channels. Figure 5 shows these data for each of the two SPRTs for the pair of WTP mantles 21A-1/21A-2 as read by the DSB at 1 mA current. The WTP cell interchange occurs at approximately 13:30 on the time axis. The differences in the mean resistance values for each of the two thermometers, expressed in temperature differences, are $-41(39)$ μK for 56860103 and $-54(36)$ μK for 162D3363. The finite power dissipation of 25 μW introduces higher uncertainties (compared to the other zero-power data series) due to unknown differences in the thermal resistances between the two cells. (see section 5.2 below).

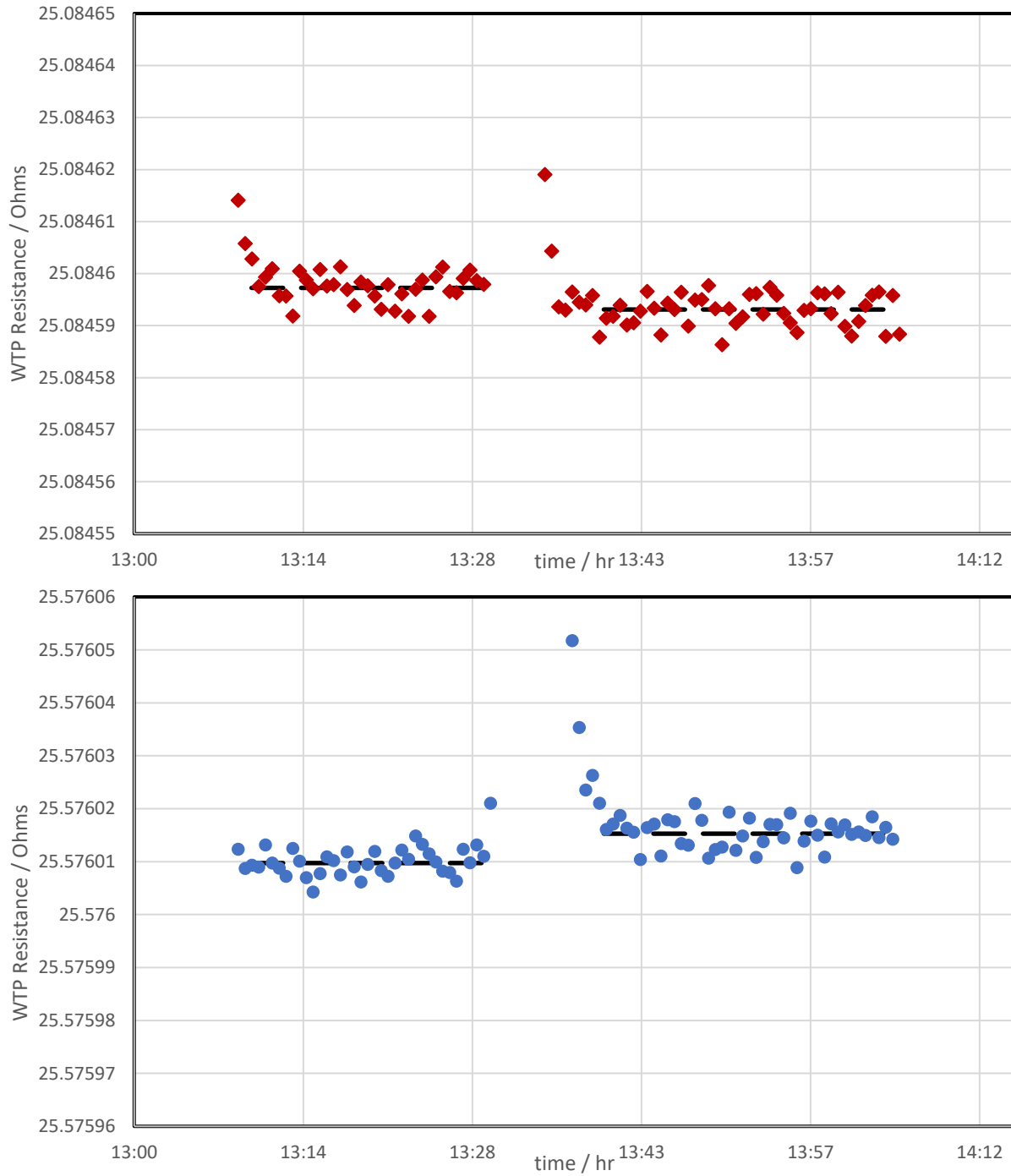


Figure 5 Time series data for Series D2 , mantles 21A-1 and 21A-2, April 9, 2021. a). SPRT 56860103 in Q1034 and later moved to 1454Q. b). SPRT 162D3363 in cell 1454Q and then moved into cell Q1034.

4.5. Data Summaries and Analysis

All unprocessed data consist of WTP resistance measurements as described in section 4.4. Average resistance values are calculated for all of the available data for each of the individual

SPRTs, with separate averages taken for the transfer cell and the reference cell. These two averages are then subtracted, ΔR , for each of the SPRT data sets. The standard deviations are calculated for all of those distributions of resistance values and combined for the statistical or type A standard uncertainty, $s(\Delta R)$, for each of those difference values. Those resistance difference values are then converted to equivalent temperature differences, ΔT , ($0.1018 \Omega/K$) for each of the SPRT's data sets. The results of those calculations are shown in Table 8 below.

Table 8 A summary of the NIST LTCF data for the differences between the transfer and reference cells.

s/n	Dates	1454Q - Q1034			
		$\Delta R / \mu\Omega$	$s(\Delta R) / \mu\Omega$	$\Delta T / \mu K$	$s(\Delta T) / \mu K$
1774092	All	-2.21	4.93	-22	49
1774096	All	-0.11	4.77	-1	48
1842385	All	-0.18	6.53	-2	65
56860103	All	-1.55	6.50	-16	65
RS163-01	All	-6.48	4.08	-65	41
RS163-04	All	3.64	3.43	36	34
56811538	21B	-6.34	3.84	-63	38
56860103	21A/D2	-4.16	3.99	-42	40
162D3363	21A/D2	-5.55	3.64	-55	36
Mean				-25	34
s-Weighted Mean				-27	39

The SPRT data shown in Table 8 is distributed slightly differently than as shown in Tables 5 and 5. The reason for this is the special nature of D2-series data from 56860103 and 162D3363 requiring those series to be split off from the other F-series and D1-series data. Hence, the D-2 series data for 56860103 is split up into a separate row from the other series data for that SPRT. This would also be the case for 162D3363, except that in that case the 18A and 19A melt data are limited to the WTP cell Q1034, and no corresponding F- or D1-series data were available for the cell 1454Q using that SPRT, leaving only the D2-series to be tabulated.

As shown in Table 8, an overall mean value may be computed for the temperature difference values. A comparison of the mean and weighted mean is also shown, where the weights are computed from the inverse square of the $s(\Delta T)$ statistics (i.e. the 's-weighted' mean). These two measures of the distribution of ΔT values yield no significant differences since there is not much difference in the $s(\Delta T)$ values themselves.

Other formulations for computing a weighted mean are better suited to the analysis of an inhomogeneous distribution of ΔT values like this. The main problem is that the number of measurements N_{ij} representing each of the i SPRTs and each of $j=1$ to 2 WTP cells are not evenly distributed, as shown in Table 6. We formulate a geometric-mean measurement number (GMMN)-weighted mean to account for this asymmetry in the ΔT distribution by creating a set of weights for the SPRT data average ΔT values from Table 8 as $w_{gmi} = (N_{i1} N_{i2})^{1/2}$, where $i=1$ to 9 for the nine rows in the table. In this formulation the minimum value for w_{gmi} is 1 and larger values are derived for data sets with larger measurement numbers for both of the WTP cells.

Table 9 lists the weighting parameters for the GMMN-weighted mean and its standard deviation of the weighted mean.

Table 9 The GMMN-weighted mean parameters for averaging the SPRT data.

s/n	Dates	1454Q - Q1034			
		Ni_1	Ni_2	W_{gmi}	$\Delta T/\mu K$
1774092	All	5	4	4.47	-22
1774096	All	6	2	3.46	-1
1842385	All	7	2	3.74	-2
56860103	All	6	3	4.24	-16
RS163-01	All	2	1	1.41	-65
RS163-04	All	2	1	1.41	36
56811538	21B	1	1	1.00	-63
56860103	21A/D2	1	1	1.00	-42
162D3363	21A/D2	1	1	1.00	-55
					-17
GMMN-weighted mean(std. dev.)					(26)

The result of the GMMN-weighted mean of the cell temperature differences is $-17(26) \mu K$. This estimated mean is well within the estimated uncertainty bounds of the other conventional estimated means from Table 8. The influence of the weighting of the first four SPRTs in the table accounts for the less negative estimated mean. The associated uncertainty estimate of $26 \mu K$ is lower than those of the other estimates, but similar to what would be calculated using a rectangular distribution model for the average ΔT values (i.e. $29 \mu K$). One aspect of Table 9 of note is that the sum of the GMMN's given are slightly different from shown in Table 6. In fact, for the cell 1454Q we have $\sum Ni_2 = 16$, which is the same as in Table 6. But for cell Q1034 we have $\sum Ni_1 = 31$, which is 8 less than that shown in Table 6. The reason for this difference is that 8 of the series F and D1 measurements for the SPRT 162D3363 are from cell Q1034 alone, and not contributing to a temperature difference.

The two main weaknesses in these data are 1.) the small value for the GMMN for the cell 1454Q and 2.) the highly extended time period of 5 years from which the data are extracted. The later of these issues can be examined further by splitting the data series into two halves, with the first half originating prior to the 2020 data lapse and the second half taken from after the 2020 data lapse. This allows for the detection of some possible drifts in the SPRTs, or in the cells themselves. In the same way, possible changes that occurred during the Covid-era facilities shutdown might be revealed. Tables 10 and 11 provide the summaries obtained when splitting up the data in this way. This splitting of the data series has the effect of culling some of the data, depending on which SPRT is considered, due to time-dependent asymmetries in the data.

Table 10 is a summary of the data presented in Table 8, except now parsed into the two time segments (i.e prior to and after 2020). As can be seen in Table 10, two of the original 8 SPRTs are removed since those data do not contain complete pairs of cell data in either of the two time segments. In addition, only two of the SPRTs (1774092 and 56850103) have sufficient data to be included in both time segments. The time-segmented ΔT data from 1774092 are entirely

consistent with that derived from the combined data set for that thermometer and with means from all of the SPRTs. The time-segmented F-series ΔT data from 56860103, however, are noticeably different, and show a strong departure from the mean values from Table 9 and from the means taken from all of the SPRTs. These data were subject to mantle stress, since measurements on both of the cells were taken only 48 hours after the 21B mantel initiations.

Table 10 A parsing of the data into two halves before and after the 2020 data lapse.

s/n	Dates	1454Q - Q1034			
		$\Delta R / \mu\Omega$	$s(\Delta R) / \mu\Omega$	$\Delta T / \mu K$	$s(\Delta T) / \mu K$
1774092	< 2020	-2.23	3.81	-22	38
1774092	> 2020	-2.74	5.89	-27	59
1774096	< 2020	-1.17	4.65	-12	47
1843485	> 2020	2.67	9.74	27	97
56860103	< 2020	-5.99	5.16	-60	52
56860103	> 2020	7.32	5.36	73	54
56811538	> 2020	-6.34	3.84	-63	38
56860103	21A/D2	-4.16	3.99	-42	40
162D3363	21A/D2	-5.55	3.64	-55	36
Mean	< 2020			-31	25
s-Weighted Mean	< 2020			-28	23
Mean	> 2020			-15	54
s-Weighted Mean	> 2020			-32	48

The simple mean and s-weighted means are shown for both time segments in the bottom four rows of Table 10. These estimates for the two time segments (i.e. before and after 2020) are not significantly different from each other, nor different from those in Table 8, as derived from the entirety of the time series. As in the case for Table 8, the uncertainties in the simple and s-weighted means are calculated as the corresponding standard deviations of the segmented data.

Table 11 is another summary of the time-segmented data as presented in Table 10, except now presented in a format analogous to that of Table 9 and used to determine a GMMN-weighted mean of the cell temperature differences. The data culling effect is noticeable from the N_{ij} values compared to those shown in Table 10, again due to the time-dependent asymmetries in the data causing an absence of suitable pairing of the cells in the more limited time segments. For the segment < 2020, we have $\sum N_{i1}=14$ for cell Q1034 and $\sum N_{i2}=6$ for cell 1454Q. For the segment > 2020, we have $\sum N_{ij}=7$ for both cells. This represents a loss of 10 data points (31–21) for Q1034 and 3 data points for cell 1454Q (16–13) when compared to the results shown in Table 9 for the full 5-year time duration.

The difference between the GMMN-weighted means for the two time segments as shown in the bottom two rows of Table 11 are more pronounced than those shown for either the simple mean or the s-weighted mean in Table 10. This difference of 25 μK , however, is still not significant relative to the uncertainty in those values as reflected in the standard deviations of

the two segmented weighted means. The uncertainties as discussed in section 5.2 include allowances for time-dependent instability in both the SPRTs and in the cells themselves.

Table 11. The GMMN-weighting parameters for averaging the time-segmented SPRT data.

s/n	Dates	1454Q - Q1034			
		N_{i1}	N_{i2}	w_{dfi}	$\Delta T/\mu\text{K}$
1774092	< 2020	4	3	3.46	-22
1774092	> 2020	1	1	1.00	-27
1774096	< 2020	6	1	2.45	-12
1842385	> 2020	1	2	1.41	27
56860103	< 2020	4	2	2.83	-60
56860103	> 2020	2	1	1.41	73
56811538	> 2020	1	1	1.00	-63
56860103	21A/D2	1	1	1.00	-42
162D3363	21A/D2	1	1	1.00	-55
GMMN-weighted mean	< 2020				-32 (25)
GMMN-weighted mean	> 2020				-7 (56)

Overall, the GMMN-weighted mean of $-17(26)$ μK from Table 9 appears to be the best estimate of the observed (uncorrected) difference in the WTP realization temperatures of cells 1454Q and Q1034 based on all of the available data as presented in this report.

5. Linking the NIST comparison data to the CCT-K7.2021 results

The data from the NRC on the NIST cell 1454Q established the difference between this NIST replacement transfer cell and the reference temperature as used for the comparison (i.e the 'Pilot Reference'). Using the notation similar to that used for the K7.2021 report [2], this is the temperature difference $T_{\text{NIST-xfer}} - T_{\text{PilotRef}} = 25.2(9.3) \mu\text{K}$ that is calculated in section 3.3 of this report based on the data shown in the K7.2021 report. This may then be combined with the difference between the K7.2021 KCRV and the pilot reference temperature, $T_{\text{KCRV}} - T_{\text{Pilot Ref}} = 4.7(7.2) \mu\text{K}$, which is a principal result from that comparison. In turn, those differences may be further combined with the NIST data presented in the previous section representing the difference between the two NIST cells 1454Q and Q1034, $T_{1454\text{Q}} - T_{\text{Q1034}} = -17(26) \mu\text{K}$, yielding a value for the difference between the NIST reference cell and the K7.2021 KCRV, $T_{\text{Q1034}} - T_{\text{KCRV}} = 38(29) \mu\text{K}$, subject to any relevant corrections and additional sources of uncertainty. The corrections are those necessary to adjust the value for $T_{1454\text{Q}} - T_{\text{Q1034}}$ for hydrostatic effects and isotopic effects, and those are described in the following section.

5.1. Corrections

The temperature corrections applied are those necessary to properly adjust the reference cell to a state consistent with the WTP definition as stated in the CCT Mise-en-Pratique for the kelvin. [17] In this case, these corrections would apply to the NIST reference cell Q1034. The transfer cell does not have any similar corrections applied since its role is to transfer a temperature difference and not define an absolute temperature, although the magnitude of such corrections are known and may still be of interest in the discussion of the results. Some small caveats to this generalization are recognized and are discussed below.

5.1.1. Hydrostatic Head

The hydrostatic head correction (HHC) as discussed in section 2.1 is applicable to all WTP cells and is also very close in magnitude between all of the standard cells types used in the K7.2021. The pressure head depths associated with each cell in the partially frozen state with a typical ice mantle is very similar among all of the K7.2021 WTP cells and any associated corrections in the observed temperature difference between two given cells would be small, or $\sim 2\%$ or less of the nominal $180 \mu\text{K}$ correction. Nominal HH depth measurements were recorded for every cell in the K7.2021 study, and the resulting small corrections were applied to the comparison data. The K7.2021 uncertainty budget includes an estimated uncertainty in these depth measurements of about $3 \mu\text{K}$, equivalent to about 1.7% or about 4 mm out of a nominal 245 mm effective pressure head. Hence, the likely difference in the HHC between cells is comparable to or less than the nominal uncertainty in determining the correction.

The actual differences in the pressure head in practice also depends on the exact model of the SPRT in use during the realization and or comparison measurement. Since we have a variety of SPRT types in use for this study, there are several different combinations of SPRT and cell in play when considering the variation of pressure heads. We have measured all of the

dimensional parameters associated with these combinations and have concluded that all such depth variations are within the nominal bounds of ± 5 mm or less (i.e. about ± 2 % in a nominal 245 mm depth) for the combinations of SPRT and cells described in section 4. For this reason, we elect to not apply any HHCs to our comparison data presented in section 4, but rather include an uncertainty of 2 % of the nominal correction (i.e. 3.7 μ K). We can state that in all cases in practice, the pressure head is between 240 mm and 250 mm with a standard uncertainty of about 1 % in any given SPRT/cell combination’s depth. An immersion profile for the transfer cell can be found in Appendix A.

5.1.2. Isotopic corrections

The K7.2021 protocol states that isotopic information (if known), pertaining to the water of the national reference cell of each participant, should be provided. There is no similar requirement for the transfer cell since this isn’t needed given its role in the comparison. Table 12 provides the results of independent isotopic assays taken from water samples associated with both of the NIST WTP cells studied in this report.

Table 12 Isotopic information for the NIST transfer and reference WTP cells.

Serial no.	Role	δD , ‰	$u(\delta D)$, ‰	$\delta^{18}O$, ‰	$u(\delta^{18}O)$, ‰	ΔT / μ K	$u(\Delta T)$ / μ K
1454Q	Transfer	4.83	1.75	18.96	0.05	15.2	1.2
Q1034	Reference	-2	2	-1.5	0.2	-2.3	1.4

The isotopic analyses for these cells are those as reported by two separate laboratories under entirely separate and private contracts with the two manufacturers of these cells. The results are provided here for completeness and we cannot verify any of the data. In the case of the 1454Q water, a private analytical laboratory (‘L1’) used continuous-flow isotope ratio mass spectrometry (IRMS) using commercial analytical equipment designed for precision isotope ratio measurements. In the case of the Q1034 water, a public university laboratory (‘L2’) used a commercial wavelength-scanned cavity ring-down spectrometer (CRDS) to determine the isotopic content of a vaporized water sample. The uncertainties shown in Table 12 are those provided by these laboratories. The reports of analysis may be found in the Appendices B and C.

Several observations are worth mentioning from the data shown in Table 12. First, the values shown for the Q1034 sample are consistent with typical terrestrial precipitation (i.e. ‘meteoric’) in the sense that the δD and $\delta^{18}O$ values are close to colinear with the GMWL, $\delta D = 8.0 \delta^{18}O + 10$ (when both quantities are expressed in the customary ‘per mil’ unit, ‰) [13]. In contrast, the values as reported for 1454Q are not consistent with meteoric waters, since the degree of relative enrichment in the ^{18}O content is far in excess of the relative enrichment in D. This anomaly suggests that the source water was prepared in a laboratory using at least one isotopically altered water source or that the source was pumped down to a pressure below its saturated vapor pressure at some point during the preparation. The K7.2021 protocol refers to this type of sample as ‘spiked’. The distinction is important since it is well known that the simplified expression for the isotopic correction in the triple point temperature as shown in Eqn 2 is less accurate in such isotopically altered waters since the assumed correlation between

$\delta^{17}\text{O}$ and $\delta^{18}\text{O}$ is no longer valid. In this case a more complicated correction equation is needed that includes the measured value for $\delta^{17}\text{O}$, but this value is not available from these reported isotopic assays.

Second, we note that the predicted temperature difference between the two cells, due to difference in their isotopic contents is $+17.5(1.8) \mu\text{K}$ whereas the measured temperature difference from Table 9 is $-17(26) \mu\text{K}$. This discrepancy of $-35(26) \mu\text{K}$, while not significant from the standpoint of the measurement uncertainty, is still an indication that other factors, such as chemical shifts in the WTP temperature (e.g. dissolved impurities, etc.), could be of the same magnitude as the isotopic shifts, and therefore masking the isotopic shifts. This has some impact on the uncertainty budget described in the following section.

Another issue concerns the experience at the NRC with isotopic analyses of a large collection of WTP cells of relevance to this study [33]. Dedyulin and Peruzzi collected isotopic composition data for 17 fused-silica and borosilicate WTP cells in 2021 to 2022. Of those cells, two had isotopic results reported from the same two laboratories that provided results to the cell manufacturers as mentioned above and also results from a third laboratory ('L3') at the University of Ottawa utilizing IRMS techniques. Dedyulin and Peruzzi found significant discrepancies in the results from one of those cells with a serial number (Q1049) close to that of the NIST reference cell (Q1034) when comparing the results of the CRDS at L2 from those of the IRMS at L3. This discrepancy amounted to a temperature difference equivalent of $9.3(1.9) \mu\text{K}$ with L3 reporting a more depleted (lighter) water result and the two labs reporting very similar uncertainties. Dedyulin and Peruzzi also found a $-13(2) \mu\text{K}$ discrepancy between the results for a different cell between isotope data reported from laboratories L1 and L3. However, they found a high degree of consistency between the L3 IRMS results of nominally identical water samples taken from separately submitted ampoules [33].

From Table 12, the as-measured value for $T_{\text{Q1034}} - T_{\text{KCRV}}$ is subject to a small nominal isotopic correction of $2.3 \mu\text{K}$ for the (as-reported) slight depletion of heavier isotopes in the Q1034 water relative to those of V-SMOW. This yields a V-SMOW corrected value for the difference $T_{\text{Q1034}} - T_{\text{KCRV}} = 40(32) \mu\text{K}$. In principle the cell temperature for 1454Q could also be corrected, but this is not necessary for the purposes of the K7.2021 comparison.

5.2. Uncertainties

The overall uncertainty budget for the purposes of the K7.2021 is structured in two parts, as shown in Table 13. The first part contains those uncertainty components relevant to the realization of the WTP using the 'National Reference Cell'. For the purposes of this more limited study, the reference cell Q1034 is designated the 'NIST/LTCF reference cell'. The second half of the uncertainty budget pertains to the Transfer cell comparison with the reference cell as carried out by the participants in any of the various NMI's laboratories. For the purposes of this study, this section of the uncertainty budget pertains to the measurements described in section 4 above for determining the difference $T_{1454\text{Q}} - T_{\text{Q1034}}$. The uncorrelated 'root-sum-squared' (RSS) uncertainty for each of these two parts is shown at the bottom of Table 13 along with the total combined standard uncertainty for both parts.

The full uncertainty budget for this study is shown in Table 13 using the nominal K7.2021 two-part structure and format. In addition, the uncertainties are further divided into three columns according to the specific data series (F, D1 or D2) as described in section 4.4. These data-series differences are only present in the LTCF measurements for the comparison portion of the uncertainty budget. Furthermore, the differences in the data-series-specific uncertainty components are only significant in a few cases.

It should be noted that the uncertainties associated with the quoted cell temperature differences in the first paragraph of section 5 above are purely statistical in nature, and do not include the additional sources of uncertainty outlined below.

5.2.1. Reference Cell Realization Uncertainty

The following text addresses each of the row entries in Table 13 for the uncertainties associated with the properties of the (national) reference cell.

5.2.1.1. Impurity Content

The LTCF reference cell, s/n Q1034, is a fused-silica glass envelope type C design purchased in 2013 (see Table 3). There is no information available pertaining to chemical impurities and there is no evidence of any air in the cell. Given the very small degree of isotopic depletion as reported for this cell, together with the fact that it yields a relatively high realization temperature with respect to other reference cells as reported in the K7.2021, there is no evidence of melting depression from chemical impurities. The estimated uncertainty component for the chemical impurity content of 10 μK as listed in Table 13 is derived from guidance from the CCT pertaining to high quality new fused-silica cells [28].

5.2.1.2. Isotopic Composition

An isotopic correction for the reference cell has been made to the V-SMOW composition based on the manufacturer's certificate of conformance and the L2 CRDS results as reported and copied to Appendix C. But given the observed discrepancies between CRDS and IRMS found by Dedyulin and Peruzzi (described in the previous section), together with the lack of consistency between the predicted and as-measured difference $T_{1454\text{Q}} - T_{\text{Q1034}}$, we have reason to assume that some additional systematic uncertainty could be in play that dominates those uncertainties (see Table 12) as reported in the L2 report of analysis for the isotopic content of Q1034. Hence, we include an additional 9 μK type B uncertainty component added to the as-reported temperature correction uncertainty from the CRDS results. When added in quadrature, the combined standard uncertainty for the isotopic correction (see Table 13) is ~ 7 times greater than that derived from the CRDS results alone (see right-hand column in Table 12). This augmentation is our attempt to address the apparent discrepancies in the corrections as found in this study and similar issues identified in the literature [33]. The origins of these discrepancies are unknown, but could be due to any number of different effects in the sample

preparation process such as sampling errors, incomplete mixing, accidental fractionation effects, etc.

5.2.1.3. Residual Gas Pressure

In some WTP cells, estimates of the residual air pressure are possible via a visual comparison of the size of a trapped gas bubble in an extension arm of the cell under both normal and inverted orientations of the cell with respect to the local vertical.[34] Unfortunately, the residual gas pressure in the reference cell is impossible to measure using this technique due to the absence of a suitable extension tube in the Type C glass envelope. We use the 1 μ K estimate based on guidance from CCT guidance derived from the use of high quality cells of different designs.

5.2.1.4. Reproducibility between realizations

The uncertainty for ‘Reproducibility between realizations’ is supposed to capture all of the sources of variability that may occur from one ice mantle to the next under normal conditions. In the case of this study, where mantle aging times were as short as 2 days, the main source of variability is due to residual crystal strains in the solid phase ice [22]. Not all of the measurements in this study were made in such a short time after mantle preparation, but the practice of putting the cell into service two days after the initial mantle formation is not uncommon within the LTCF due to limitations on the available time to perform needed measurements. We account for these effects with an estimated standard uncertainty of 30 μ K based on our experience over 17 years of collecting WTP resistance data on capsule SPRTs within the LTCF and analyzing those statistical distributions.

5.2.1.5. Heat flux perturbations

The component identified as ‘heat flux perturbations’ represents departures from phase and temperature equilibrium within the WTP cell’s interior volumes, including the thermowell and SPRT, due to heat transport across regions of the cell’s volume. The magnitude of any heat flux is primarily limited by the thermal characteristics of the maintenance system, in this case a stirred water bath. The effect of any heat flux is mitigated by the degree of immersion of the SPRT into the thermowell together with the spatial distribution of the solid-liquid interfacial areas within the cell. In practice, stray and or variable heat flux is negligible when a precision-controlled water bath is used to maintain the mantle(s) of the cells, with a suitable SPRT immersion depth, and when the mantle is properly formed with an inner melt along the thermowell boundary. The cells are kept well below the surface of the bath water-ethanol mixture and temperature control is sufficient to limit short term fluctuations in temperature to within ± 1 mK of the nominal set point. The set point itself is determined by placing an SPRT into the bath fluid volume and comparing the reading to the as-realized WTP resistance for that SPRT. The SPRT immersion profile has customarily been used to estimate the uncertainty due to heat flux perturbations in fixed point cells, but this statistical metric alone may underestimate the magnitude of actual effects in practice. We adopt the consensus value of 5 μ K based on the experience from the K7 comparison [3].

5.2.1.6. Hydrostatic Head Correction

The hydrostatic head correction is subject to an uncertainty due to the uncertainty in determining the head depth. As already discussed in section 5.1.1 above, there is uncertainty in the $\sim 180 \mu\text{K}$ nominal correction of 2 %, or $3.7 \mu\text{K}$.

5.2.2. Transfer cell comparison uncertainty

5.2.2.1. Single mantle repeatability

The single mantle repeatability uncertainty is meant to capture all of the random or quasi-random effects that produce short term fluctuations in the reading of the SPRT for a single ice mantle realization. For this treatment we limit the category to the noise-equivalent temperature from the SPRT measurement instrumentation and treat other purely thermal fluctuation sources separately. This uncertainty component corresponds, in principle, to the uncertainties for the cell temperature difference values already quoted above.

The achievable voltage noise in the F-series bridge instrument as installed in the LTCF is typically between 1 nV to 2 nV rms. The contributions from current noise are negligible in comparison. Using 1 mA to 2 mA excitations, the signals are between 25 mV and 50 mV, leading to a range of noise of $10 \mu\text{K}$ to $20 \mu\text{K}$ at finite current or about $(14 \text{ to } 27) \mu\text{K}$ when extrapolated to zero-power. The values that appear in Table 13 are derived from pooled standard deviations of SPRTs in situ and are slightly higher than these noise estimates. The difference is likely caused by induced noise in the SPRTs from alternating stray magnetic fields associated with the close proximity to motors operating in the stirred water bath. The values for the D-series measurements are slightly higher than those from the F-series.

5.2.2.2. Reproducibility of separate mantle realizations

The transfer cell has the same $30 \mu\text{K}$ uncertainty component for ‘Reproducibility of separate mantle realizations’ as described in section 5.2.1.4 above for the reference cell.

5.2.2.3. Reproducibility for different types of SPRTs

The uncertainty component designated ‘Reproducibility for different types of SPRTs’ is used to account for the use of multiple SPRTs and the extended time duration of 5 years taken for the purposes of this study. This was the most significant departure from the original K7.2021 protocol, but it was necessary in order to collect enough data for the analysis. As described in section 4.1, we used a collection of 7 different capsule-type SPRT and one other long-stem SPRT in the study. Of those 8 SPRTs listed in Table 5, there are five distinct types or models. All of these are equally capable of achieving a nominal short-term repeatability of $\sim < 20 \mu\text{K}$ when equilibrated in a WTP cell using the resistance bridge instrumentation described in section 4.4 above. Over longer term use, however, we cannot rule out somewhat larger changes taking place in the SPRT resistance over time. But there are well established upper limits in stability

that we can use to estimate a rectangular ('brick wall') distribution of WTP resistance values of $\pm 100 \mu\text{K}$. From this limit we estimate a standard uncertainty for possible SPRT instability of $200 \mu\text{K} / (12)^{1/2} = 58 \mu\text{K}$.

5.2.2.4. Hydrostatic Head Correction

As already discussed in section 5.1.1 above, there is uncertainty in the $\sim 180 \mu\text{K}$ nominal correction of 2 %, or $3.7 \mu\text{K}$.

5.2.2.5. Self Heating Effects

The uncertainty in the self-heating correction ('zero-power) is estimated to be 1 % of the correction for the F-series measurements and 2 % for the D1 series. The reason for the higher uncertainty in the D-series is due to the way in which the correction is performed using the DSB's built-in instrument firmware.

In the case of the D-2 series, there is no correction and the variations in the external component of the self-heating (ESH) come into play. Specifically, the measurement is susceptible to any difference in the ESH when immersed in one of the cells versus the other. The observed self-heating coefficient is the sum of the internal and external contributions. The internal contribution is a characteristic of the specific SPRT and the external contribution is installation dependent, as produced by the sum of various thermal resistances over multiple external interfacial boundaries.[24] Variations in the ESH will therefore lead to errors when comparing the cell's apparent temperature. We have estimated the magnitude of these variations through experimental distributions in self-heating coefficients from two of the SPRTs listed in Table 6. We estimate that the ESH coefficient is $4(1) \mu\text{K}/\mu\text{W}$ for the two SPRTs used in the D-2 series measurements. For the 1 mA excitation level, the $25 \mu\text{W}$ power dissipation then produces an uncertainty of $25 \mu\text{K}$ for the D-2 series.

5.2.2.6. Standard Resistor

The standard resistors exhibit small short-term resistance fluctuations due to their small temperature coefficients coupled with the thermal variations associated with their temperature control enclosures. The F-series and D-series instruments use separate thermostated standard resistors which lead to different uncertainties in practice. Longer term drift effects in the resistance values for the standard resistors are also in play due the extended duration of the study.

In the case of F-series measurements, the standard resistor can exhibit significant short-term temperature variations from the limited degree of control ($\pm 0.1 \text{ }^\circ\text{C}$) for the air bath enclosure installed in the LTCF. However, for most all of the measurements included in this study, real-time temperature corrections are applied to the standard resistor (100Ω , s/n 268185, $\alpha = -0.4 \mu\Omega/\Omega \cdot ^\circ\text{C}$ at $25.0 \text{ }^\circ\text{C}$). This reduces the effective uncertainty to a negligible level, or approximately $1 \mu\text{K}$ for the F-series measurements. Longer term drift in this standard resistor has fairly strict limits due to its exceptional stability, with quality records indicating a fractional

change of $0.0(0.1) \mu\Omega/\Omega$ observed over a 27 year history. This implies a drift rate uncertainty of $0.019 \mu\Omega/\Omega$ over a 5 year time interval, leading to a temperature equivalent uncertainty for drift of $5 \mu\text{K}$. The short-term and longer-term effects are added in quadrature for a combined standard uncertainty of $5 \mu\text{K}$ due to standard resistor instability.

In the case of the D-series measurements, the control stability of the standard resistor (25Ω , s/n 267924, $\alpha = 1 \mu\Omega/\Omega \cdot ^\circ\text{C}$ at $27.7 ^\circ\text{C}$) is approximately ($\pm 0.05 ^\circ\text{C}$), leading to an uncertainty of $13 \mu\text{K}$. The longer-term drift limits for this standard resistor are similar to that of the 100Ω with a history over 25 years indicating changes of $0.0(0.1) \mu\Omega/\Omega$. The long-term drift uncertainty of $0.02 \mu\Omega/\Omega$ in resistance then translates to a $5.5 \mu\text{K}$ uncertainty in temperature. The short-term and longer-term effects are added in quadrature for a combined standard uncertainty of $14 \mu\text{K}$ due to standard resistor instability for the D-1 series measurements. The D-2 series measurements were only made under short-term conditions, so the long-term component is not added in that case, leaving a $13 \mu\text{K}$ uncertainty in that case.

5.2.2.7. Bridge uncertainty

The comparison uncertainty contributions from the resistance bridge instrumentation are limited to fine-scale differential non-linearity only. For the F-series measurements, this results from the last few least-significant digits as interpolated across adjacent IVD windings using an ADC. The least significant bit for the ADC is 5×10^{-9} in the measured ratio, or the equivalent of $5 \mu\text{K}$. For the D-series measurements, we rely on the DSB instrument specification for non-linearity in a narrow range near ratios of 1.0, which is the equivalent of $17 \mu\text{K}$ for 25.5Ω SPRTs.

5.2.2.8. Heat Flux perturbations

The heat flux uncertainty contribution for the transfer WTP cell measurements is identical to that already described in section 5.2.1.5 above for the reference cell, or $5 \mu\text{K}$.

Table 13 Uncertainty budget for this study in the K7.2021 format of standard uncertainties.

	F Series	D1 Series	D2 Series	
Description	u/ μK	u/ μK	u/ μK	Comment
NIST/LTCF Reference Cell:				
Impurity Content	10			estimated by CCT Guide
Isotopic Content	9.1			Additional 9 μ K Type B added
Residual Gas pressure	1.0			typical upper limit
Reproducibility between realizations	30			assuming only 2 d aging time
Heat flux perturbation	5			realized in precision water/ethanol bath
HH effect correction	3.7			estimated at 5 mm unc. of head
Transfer Cell Comparison:				
Repeatability of single mantle realization	27	37.5	27.5	typically observed standard deviations
Reproducibility of separate mantle realizations	30			effect of age of mantle
Reproducibility for different types of SPRTs	58			SPRT stability over years timeframe
HH effects	3.7			estimated at 2% of correction
Self-heating effects	6.5	13	25	Zero-power correction or ESH (see text)
Standard Resistor Stability	5	14	13	RMS thermostat stability
Bridge Uncertainty	5	17	17	diff. non-linearity over restricted range
Heat Flux Perturbations	3.7			
RSS Nat Ref Cell	33.5	33.5	33.5	
RSS Transfer Cell Comparison	71	80	78	
Combined Standard Uncertainty	79	86	85	

5.3. Final Results and Discussion

The results for this study are summarized in Table 14 in terms of the principal temperature differences and their associated uncertainties. The first row is the result described in section 3.3 based on the NRC K7.2021 comparison data for the NIST replacement transfer cell 1454Q relative to the average temperature for the NRC pilot reference cells as published in the final report [2]. The second row is the result of the K7.2021 for the KCRV relative to the pilot reference cells.

Table 14 A summary of the temperature difference results obtained for this study.

K7.2021				
Row	Difference	$\Delta T/\mu\text{K}$	$u(\Delta T)/\mu\text{K}$	Comment
1	$T_{1454\text{Q}} - T_{\text{PilotRef}}$	25.2	9.3	NRC Data
2	$T_{\text{KCRV}} - T_{\text{PilotRef}}$	4.7	7.2	K7.2021 Result
3	$T_{1454\text{Q}} - T_{\text{Q1034}}$	-17	71	NIST Data, GMMN weighted Mean (Table 9)
4	$T_{1034\text{Q}} - T_{\text{KCRV}}$	37.8	72.2	Uncorrected
5	$T_{1034\text{Q}} - T_{\text{VSMOW}}$	-2.3	9.2	Isotope Correction for Q1034
6			33.5	NIST/LTCF WTP realization Uncertainty
7				
8	$T_{\text{LTCF}} - T_{\text{PilotRef}}$	44.7	79	As corrected to VSMOW
9	$T_{\text{LTCF}} - T_{\text{KCRV}}$	40.0	80	As corrected to VSMOW

The third row in Table 14 is the principal result of this study for the direct temperature difference between the NIST transfer cell and reference cell as described in section 4. The result is taken from Table 9 using the GMMN-weighted average of all of the available temperature difference data. The 71 μK uncertainty in the result is taken from the ‘RSS Transfer Cell Comparison’ uncertainty as calculated in section 5 and shown near the bottom of Table 13. The uncertainty specific to the F-series measurements is used based on the fact that the majority of the data are from the F-series. As previously mentioned in section 4.2, this result of $-17(71) \mu\text{K}$ may be compared to the result of $-24(23) \mu\text{K}$ as shown in Flowers-Jacobs *et al.*[31], for these same two cells. In that earlier work, only the 17A and 17B data from SPRT 1774092 was available, and the uncertainty of 23 μK was limited to a statistically derived uncertainty of the weighted mean. Given this partially-common-data connection between these two results, good agreement would be expected.

The fourth row of Table 14 is a temperature difference between the NIST reference cell, Q1034, and the K7.2021 KCRV. This result is derived from the other results shown the Table using row 1 minus row 2 minus row 3. The 72 μK uncertainty is the RSS combined uncertainty for those row’s temperature differences. The result does not include the correction for isotopic content in the Q1034 reference cell.

In the fifth row of Table 14 the isotopic correction is given for the NIST/LTCF reference cell, Q1034. This correction is based on the isotopic content for a water sample identified in the

Report of Analysis (see Appendix C) from the L2 laboratory using methods based on a commercial CRDS instrument. As already mentioned in section 5.2.1.2 above, the uncertainties have been increased by a factor of 4 from those found in that report.

The sixth row of Table 14 restates the realization uncertainty of 33.5 μK for the reference cell, Q1034, as found in Table 13. This uncertainty is then included in the calculations of the combined uncertainties for the final two composite temperature differences found in rows 8 and 9 of Table 14. This includes those uncertainty components associated with the realization of the water triple point as defined. (Note: Row 7 of Table 14 is left blank intentionally.)

The derived temperature difference $T_{\text{LTCF}} - T_{\text{PilotRef}}$ is the NIST/LTCF reference cell temperature as corrected to a VSMOW composition (T_{LTCF}) minus the K7.2021 Pilot Reference cells (T_{PilotRef}), as shown in row 8 of Table 14. This difference is calculated from the result in row 1 and subtracting the results in row 3 and row 5. The 79 μK combined uncertainty for this result is calculated as the RSS of the uncertainties given in rows 1, 3 and 6 of the table. The isotopic correction uncertainty of 9.2 μK combined in row 5 is excluded since this is already included in the row 6 realization uncertainty. Finally, the similar result shown in row 9 for $T_{\text{LTCF}} - T_{\text{KCRV}}$ is the difference between the results from row 4 and row 5. The associated uncertainty in this case is practically indistinguishable from that of row 8, being derived as the RSS of the uncertainties in rows 4 and row 6. The only difference between these two uncertainties is the contribution of the 4.7 μK uncertainty for the KCRV as given in row 2.

It should be noted that the result of row 8 for $T_{\text{LTCF}} - T_{\text{PilotRef}} = 45 \mu\text{K}$ is higher than all but one of the national reference cells of the 15 NMI participants of the K7.2021 comparison. In addition, NRC data indicate that the NIST transfer cell yielded the highest temperature of all the transfer cells submitted for the K7.2021 comparison (compare the 25 μK value in row 1 of Table 14 with Table 4.7 in reference [2]). One possible explanation for these results could be unusually heavy isotopic compositions (enriched in heavier isotopes) for both of the NIST cells together with an inaccurate assessment of the isotopic content for the Q1034 reference cell.

From the standpoint of K7.2021 results, however, the deviations of both the NIST transfer cell temperature and the NIST/LTCF reference cell temperature are well within the nominal statistical bounds with respect to those temperature distributions. In the case of the K7.2021 transfer cells relative to the pilot reference, the distribution of the 15 cells (Table 4.7 in reference [2]) yields a mean of $-10.4 \mu\text{K}$ with a standard deviation of 25.7 μK . Thus, the result for the NIST transfer cell Q1454 of 25.2 μK is only 1.39 standard deviations from the mean.

Similarly, in the case of the national reference cells relative to the pilot reference, the K7.2021 distribution of those 15 NMIs' WTP temperatures (Table 5.1 in reference [2]) yields a mean of $-0.24 \mu\text{K}$ with a standard deviation of 28.0 μK . This translates to the NIST/LTCF reference cell 1034Q VSMOW corrected value of 44.7 μK being only 1.61 standard deviations from the mean for that distribution.

6. Conclusions

We have documented a traceability between a specific NIST WTP reference cell, Q1034, and the results of the recent K7.2021 International key comparison for WTP cells. The principal result is a value for the NIST reference WTP cell, as corrected to a VSMOW-equivalent composition, of +40(80) μK relative to the KCRV for the K7.2021. This was established and demonstrated despite the withdraw of NIST from formal participation in the K7.2021 after breakages of two NIST transfer cells that had been submitted for the purposes of that comparison. The traceability results relied on NIST data and NRC data for the NIST transfer cell Q1454, which suffered an accidental breakage at NIST in June of 2022. The results from NIST relied on a prior 5 year sampling of routine laboratory measurements associated with scale maintenance, research and quality system support activities. Those measurements allowed temperature differences to be obtained between the transfer cell and reference cell based on data taken prior to the loss of the transfer cell. The results are sufficient to establish a link to the K7.2021 KCRV and to support the NIST quality system documentation requirements.

While the NIST measurements did not conform to the measurement protocol for the K7.2021, the results are nonetheless deemed reliable within the stated uncertainties given in this study. The rigor associated with a key comparison measurement protocol such as that used for the K7.2021 is naturally much higher than what is normally achievable in routine laboratory temperature scale and quality system maintenance activities. This distinction is reflected in the 80 μK standard uncertainty from this study as compared to values ranging from 13 μK to 82 μK from the 15 participating NMIs of the K7.2021.

References

- [1] H. Preston-Thomas, (1990) The International Temperature Scale of 1990 (ITS-90), *Metrologia*, 1990, 27, 3-10.
- [2] A. Peruzzi¹, S. Dedyulin¹, M. Levesque¹, D. del Campo, B.C. Garcia Izquierdo, M.E. Gomez, K.N. Quelhas, M.A.P. Neto, B.M. Lozano, L. Eusebio, I. Yang, F. Sparasci, C. Martin, L. Risegari, P. Saunders, E. Molloy, X.K. Yan, J.P. Sun, X.J. Feng, J.T. Zhang, M.-K. Ho, T. Nakano, J.V. Widiatmo, I. Saito, E. Ejigu, J. Pearce, S. Rudtsch, L. Buenger, M. Kalemci, A. Uytun, C. Bruin-Barendregt, M. Panman, D.R. White, A. Possolo (2023) CCT-K7.2021:CIPM Key Comparison of Water-Triple-Point Cells CCT-K7, *Metrologia* 60 03002 <https://iopscience.iop.org/article/10.1088/0026-1394/60/1A/03002>
- [3] M. Stock et al., “Final Report on CCT-K7 Key Comparison of water triple point cells”, *Metrologia* 2006, 43 Tech. Suppl. 03001
- [4] W Wagner and A Prus (2002) The IAPWS Formulation 1995 for the Thermodynamic Properties of Ordinary Water Substance for General and Scientific Use, *J. Phys. Chem. Ref. Data* 31, 387–535 <https://doi.org/10.1063/1.1461829>
- [5] Stimson, H.F. 1945. *J. Wash. Acad. Sci.* 35: 201-217
- [6] James L Cross, Founder, Jarrett Instrument Co., Inc. (1971 to 1996). An earlier ‘doing-business-as’ name for the company was “J&J”.
- [7] Furukawa G. T. and Bigge W. R., Reproducibility of some triple point of water cells, *Temperature, Its Measurement and Control In Science and Industry*, Vol. 5, American Institute of Physics, New York (1982), p 291.
- [8] ASTM (2016) E1750
- [9] Harvey A H, McLinden M O and Tew W L 2013 Thermodynamic analysis and experimental study of the effect of atmospheric pressure on the ice point AIP Conf. Proc. 1552 221–6
- [10] Hill K D 1999 Triple point of water cells and the solubility of borosilicate glass Proc. TEMPMEKO '99: 7th Int. Symp. on Temperature and Thermal Measurements in Industry and Science ed J F Duddledam and M J de Groot (Delft: NMI-Van Swinden Laboratorium) 68–73
- [11] White D R, Downes C J, Dransfield T D and Mason R S 2004 Dissolved glass in triple-point-of-water cells Proc. TEMPMEKO '04: 9th Int. Symp. on Temperature and Thermal Measurements in Industry and Science ed D Zvizdic (Zagreb: Laboratory for Process Measurement) 251–6
- [12] S N Dedyulin et al 2020 On the long-term stability of the triple-point-of-water cells *Metrologia* 57 065032 <https://doi.org/10.1088/1681-7575/abb52f>
- [13] Sylvia Dee et al (2023) *Environ. Res.: Climate* 2 022002 DOI 10.1088/2752-5295/acbe1
- [14] J V Nicholas et al 1996 Isotopic composition of water used for triple point of water cells *Metrologia* 33 265
- [15] Comité International des Poids et Mesures 1969 The International Practical Temperature Scale of 1968 *Metrologia* 5 35
- [16] Consultative Committee for Thermometry Recommendation T1 to the CIPM, CCT/05-30(rev) “Clarification of the definition of the kelvin” (2005)

- [17] Consultative Committee for Thermometry, CCT, (2017) "Technical Annex for the International Temperature Scale of 1990 (ITS-90)", BIPM, Sevres, France.
https://www.bipm.org/utils/en/pdf/MeP_K_Technical_Annex.pdf
- [18] Faghihi V., Kozicki M., Aerts-Bijma A.T., Jansen H.G., Spriensma J.J., Peruzzi A., Meijer H.A.J., (2015) "Accurate experimental determination of the isotope effects on the triple point temperature of water. I. Dependence on the ^2H abundance", *Metrologia* 52 819-826, and (2015), "Accurate experimental determination of the isotope effects on the triple point temperature of water. II. Dependence on the ^{18}O and ^{17}O abundances" *Metrologia*, 52, 827-834.
- [19] White D R and Tew W L (2010) Improved Estimates of the Isotopic Correction Constants for the Triple Point of Water, *Int. J. Thermophys.* 31 1644-1653
- [20] Michael Stock et al (2019) *Metrologia* 56 022001. <https://doi.org/10.1088/1681-7575/ab0013>
- [21] R Pello et al (1997) Results of an international comparison of water triple-point cells, *Metrologia* 34 393
- [22] G T Furukawa, BW Mangum and GF Strouse (1997) Effects of different methods of preparation of ice mantles of triple point of water cells on the temporal behaviour of the triple-point temperatures, *Metrologia* 34 215.
- [23] Mangum, B. and Furukawa, G. (1990), Guidelines for Realizing the International Temperature Scale of 1990 (ITS-90), Technical Note 1275 (NIST TN1275), National Institute of Standards and Technology, Gaithersburg, MD,
https://tsapps.nist.gov/publication/get_pdf.cfm?pub_id=905199
- [24] Tew WL (2015) Calibration of Cryogenic Resistance Thermometers between 0.65 K and 165 K on the International Temperature Scale of 1990, NIST Special Publication 250, SP250-91.
- [25] M Zhao and GF Strouse, (2007) VSMOW Triple Point of Water Cells: Borosilicate versus Fused-Quartz, *Int J Thermophys* 28:1923–1930
- [26] GF Strouse and M Zhao, (2007) The Impact of Isotopic Concentration, Impurities, and Cell Aging on the Water Triple-Point Temperature, *Int J Thermophys* 28:1913–1922
- [27] Strouse GF (2008) *Standard Platinum Resistance Thermometer Calibrations from the Ar TP to the Ag FP* NIST Special Publication 250, SP250-81.
<https://doi.org/10.6028/NIST.SP.250-81>
- [28] A Peruzzi, E Mendez-Lango, J Zhang, and M Kalemci (2018) Guide to the Realization of the ITS-90, Triple Point of Water, CCT/ BIPM.
- [29] A Peruzzi and S. Dedyulin (2022) NRC measurement set-up and preparatory work for CCT-K7.2021 key comparison of triple-point-of-water cells *Metrologia* 59 045011 (13pp)
- [30] PJ Mohr, DB Newell, BN Taylor and E Tiesinga (2018) Data and analysis for the CODATA 2017 special fundamental constants adjustment, *Metrologia* 55 125–146
- [31] N Flowers-Jacobs, et al, (2017) The NIST Johnson Noise Thermometry System for the Determination of the Boltzmann Constant, *J Res NIST*,
- [32] W. L. Tew and G. F. Strouse, (2001) "Standard Reference Material 1750: Standard Platinum Resistance Thermometers 13.8033 K to 429.7484 K", NIST Special Publication 260-139, Dec, 2001.

- [33] S N Dedyulin and A Peruzzi (2022) No country for old borosilicate triple-point-of-water cells *Metrologia* **59** 055009
- [34] White D.R., (2004), Measuring the residual air pressure in triple-point-of-water cells, *Meas. Sci. Technol.* 15, 2004, N15-N16.

Appendix A. NIST Certificate of Analysis for the NIST transfer cell s/n 1454Q

CERTIFICATE OF ANALYSIS

International Temperature Scale of 1990

Water Triple-Point Cell
Isotech Model B13-65-270Q
Serial Number 1454

Tested for
NIST Thermodynamic Metrology Group
Gaithersburg, MD 20899

22 October 2015

22 October 2015

In reply refer to: 685/internal

NIST Thermodynamic Metrology Group
Attn: Wes Tew
100 Bureau Drive
Gaithersburg, MD 20899

Subject: Certification of a water triple-point cell
(Isotech Model B13-65-270Q, s/n 1454)
Purchase Order No.: 685.01

Dear Wes Tew,

A direct comparison of your water triple-point cell (Isotech Model B13-65-270Q, s/n 1454) was made against one of our laboratory reference water triple-point cells (s/n A-Q5009). The measurement system included an ASL Model F18 operating at a frequency of 30 Hz with a 100 Ω Tinsley Model 5685A reference resistor, temperature controlled to 298.15 K \pm 8 mK, and a 25.5 Ω SPRT. Corrections were made to account for the differences in immersion depth and for the isotopic composition of your cell and the NIST reference cell.

As shown in figure 1, the triple-point temperature of your cell is within 0.02 mK of the NIST reference cell. As given in Appendix A, the expanded uncertainty ($k=2$) of the direct comparison is 0.10 mK. As given in Appendix B, the expanded uncertainty ($k=2$) assigned to the realization of the NIST reference cell is 0.05 mK.

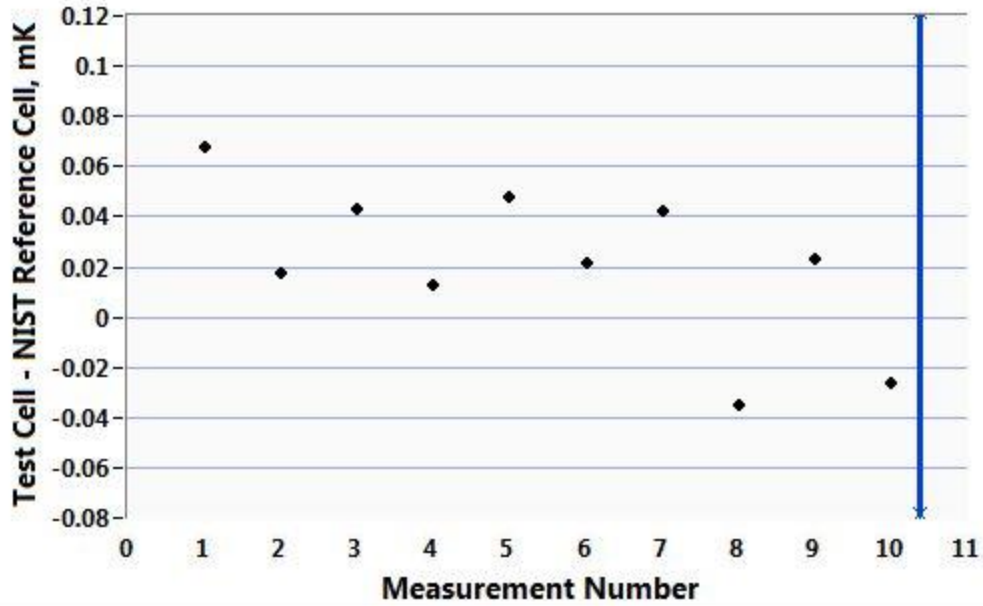


Figure 1. Direct comparison of the Thermodynamic Metrology Group water triple-point cell (Isotech Model B13-65-270Q, s/n 1454) with a NIST reference water triple-point cell (s/n A-Q5009). The vertical double ended arrow line indicates the direct comparison uncertainty ($k=2$).

Figure 2 gives an example of the immersion characteristics (heat-flux test), using a Isotech Model B13-65-270Q water triple-point cell relative to the ITS-90 assigned hydrostatic-head effect for water. A thermometer must track the hydrostatic-head effect over the bottommost 3 cm of the reentrant well to exhibit proper immersion in a fixed-point cell.

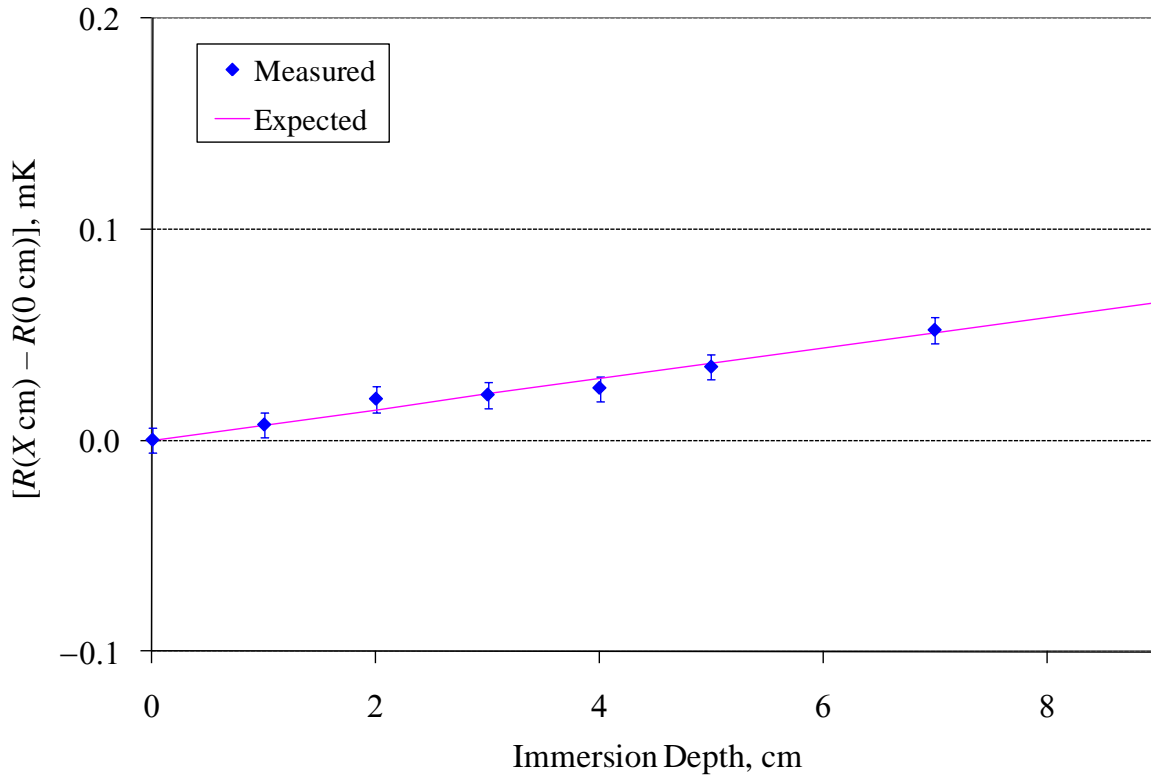


Figure 2. Heat-flux test of Isotech Model B13-65-270Q water triple-point cell using a Hart Scientific Model 5681 SPRT.

Sincerely,

Gregory F. Strouse
Leader, Thermodynamic Metrology Group
Sensor Science Division

A.1. Uncertainty budget for direct comparison of the NIST Thermodynamic Metrology Group water triple point cell (Isotech Model B13-65-270Q, s/n 1454) with one of the NIST reference water triple point cells (s/n A-Q5009)

Type A

	u_i / mK	
Bridge Repeatability	0.01	both cells
Direct Comparison Repeatability	0.03	pooled s.d. of pair differences
Total A	0.03	

Type B (rectangular distribution unless otherwise noted)

Isotopic correction	0.002	NIST cell, normal distribution
Hydrostatic-head	0.01	both cells
SPRT self-heating	0.04	both cells
Immersion (Heat Flux)	0.014	both cells, normal distribution
Gas Pressure	0.00	both cells
Total B	0.03	
Total Standard Uncertainty (k = 1)	0.05	
Total Expanded Uncertainty (k = 2)	0.10	

A.2. Uncertainty budget for the realization of a NIST reference water triple point cell (s/n A-Q5009)

	u_i / mK
Bridge Repeatability	0.002
Bridge Non-Linearity	0.02
Bridge Quadrature Effects (AC only)	0.01
Reference Resistor Resistance	0.01
Phase Transition Realization Repeatability	0.005
Chemical Impurities	0.01
Hydrostatic Head Correction	0.00
SPRT Self-Heating Correction	0.02
Heat Flux	0.003
Gas Pressure	0.00
Slope of Plateau	0.00
Isotopic Variation	0.002
	u_c 0.024
	U ($k=2$) 0.05

Appendix B. Report of Isotopic Analysis for NIST transfer cell s/n 1454Q



LABORATORY REPORT: Results Files

Client Details

Name: Isotech
Contact: Andrew Dolman
PO No. PO 15PO1178

Sample Details

Number: 1
Material: Water

Sample Tracking

IA Reference No.: 150615-2
Date of Arrival: 15-Jun-2015

Analysis Details

Isotope(s): Deuterium & Oxygen-18
Method: Equilibration IRMS
Report Date: 23-Jun-2015

Deuterium Analysis Results

Sample Identification	Result $\delta^2\text{H}$ (ppm)	Result $\delta^2\text{H}_{\text{V-SMOW}}$ (‰)	Mean $\delta^2\text{H}_{\text{V-SMOW}}$ (‰)	Std. Dev. $\delta^2\text{H}_{\text{V-SMOW}}$ (‰)
B13-65-1454	156.66	5.94		
"	156.63	5.74		
"	156.17	2.82	4.83	1.75

Quality Control Reference Standards-Deuterium Analysis

Reference Standard	Result $\delta^2\text{H}_{\text{V-SMOW}}$ (‰)
IA R053	-58.65
"	-62.19
"	-64.30
mean=	-61.71
1sd=	2.86
accepted=	-61.97
n	3

Oxygen-18 Analysis Results

Sample Identification	Result ^{18}O (ppm)	Result $\delta^{18}\text{O}_{\text{V-SMOW}}$ (‰)	Mean $\delta^{18}\text{O}_{\text{V-SMOW}}$ (‰)	Std. Dev. $\delta^{18}\text{O}_{\text{V-SMOW}}$ (‰)
B13-65-1454	2039.09	18.98		
"	2038.94	18.90		
"	2039.13	19.00	18.96	0.05

Quality Control Reference Standards-Oxygen-18 Analysis

Reference Standard	Result $\delta^{18}\text{O}_{\text{V-SMOW}}$ (‰)
IA R053	-10.09
"	-10.06
"	-10.11
mean=	-10.09
1sd=	0.02
accepted=	-10.18
n	3

Appendix C. Report of Isotopic Analysis for NIST reference cell s/n Q1034

Stable Isotope Ratio Facility for Environmental Research
Department of Biology
University of Utah
Salt Lake City, UT 84112
801 581-8917

ISOTOPE ANALYSIS REQUEST

Client: Fluke Calibration
Isotope analysis requested: hydrogen, oxygen
Date of arrival: 3/3/13
Number of samples analyzed: 1
Type of sample (water, solid, etc.): water
Type of analysis: WS-CRDS

Results:

SIRFER #	Sample #	$\delta^2\text{H}_{\text{VSMOW}}$ (‰)	‰ $\delta^{18}\text{O}_{\text{VSMOW}}$ (‰)
13-2450	5901-C-Q1034	-2	-1.5

Sample preparation

To prepare water samples for $\delta^2\text{H}$ and $\delta^{18}\text{O}$ analysis, a 400 μL aliquot of the sample is pipetted into a 1.8 mL glass gas chromatography crimpseal vial. Without special arrangements, no other preparation procedures (such as distillation) are performed. If the samples are not prepared immediately, they are placed in a cold room or frozen, thus eliminating sample evaporation.

Sample Analysis, $\delta^2\text{H}$ and $\delta^{18}\text{O}$

The prepared samples are analyzed for $\delta^2\text{H}$ and $\delta^{18}\text{O}$ using a Picarro wavelength-scanned cavity ring-down spectrometer (WS-CRDS). During this process, 1.5 μL of water is injected into an evaporation chamber and is completely vaporized. A dry stream of nitrogen gas carries the vapor into the ring-down cavity where temperature and pressure are actively monitored and stabilized. Inside the cavity, WS-CRDS uses an infrared laser and absorption spectroscopy to repeatedly measure the different isotopologues present in water and calculates $\delta^2\text{H}$ and $\delta^{18}\text{O}$ isotope ratios.

Quality Assurance, $\delta^2\text{H}$ and $\delta^{18}\text{O}$

Waters of known isotopic signatures are included in every run for normalization. These internal reference waters have been calibrated against accepted NIST water reference waters. All vials containing either internal reference water or unknown water are analyzed in duplicate during an analytical run.

Calculations

Delta values are expressed in the units of per mil (‰). One per mil unit represents a one-part-per-thousand difference from a standard and is calculated using the formula:

$$\text{Delta } (\delta) \quad \delta_{SA} = [R_{SA} / R_{ST} - 1] \times 1000$$

Where: R_{SA} is the measured isotope ratio (abundance) of the unknown sample and R_{ST} is the defined isotope ratio of the standard.

Standardization

For $\delta^2\text{H}$ and $\delta^{18}\text{O}$ measurements of water, the accepted primary standard is “Vienna Standard Mean Ocean Water” (VSMOW). The isotopic abundances of VSMOW are 0.0001558 for $^2\text{H}/^1\text{H}$ and 0.002005 for $^{18}\text{O}/^{16}\text{O}$. By definition, the isotopic composition of VSMOW has the value of $\delta = 0$ ‰ for both $\delta^2\text{H}$ and $\delta^{18}\text{O}$.

Other NIST reference waters used for calibration purposes are:

<u>Reference Material</u>	<u>Name</u>	<u>Isotopic Composition (‰)</u>
“Greenland Ice Sheet Precipitation”	GISP	-189.7 $\delta^2\text{H}$ VSMOW - 24.8 $\delta^{18}\text{O}$ VSMOW
“Standard Light Antarctic Precipitation”	SLAP	-428.0 $\delta^2\text{H}$ VSMOW - 55.5 $\delta^{18}\text{O}$ VSMOW

Explanation of results

Delta values have been normalized to international standards to account for instrument drift and temperature effects. Associated with the delta values is a listing of the uncertainty of the analysis. The uncertainty values are based on the following:

duplicate injections of each unknown water during $\delta^2\text{H}$ and $\delta^{18}\text{O}$ analysis

The uncertainty for the $\delta^2\text{H}$ analysis was ± 2 ‰ and for the $\delta^{18}\text{O}$, the uncertainty was ± 0.2 ‰.